IDENTIFYING MECHANISMS OF THYMUS AND PARATHYROID CELL FATE SPECIFICATION

by

MICHAEL NUNNELEY

(Under the Direction of Nancy Manley and Jonathan Eggenschwiler)

ABSTRACT

The thymus and parathyroid have different functions and locations in the adult body. Despite these differences, both organs arise from a common primordium in the embryo: the third pharyngeal pouch (3rd PP). A longstanding question is how cells in the 3rd PP are specified into the thymus or parathyroid. Two transcription factors, FOXN1 and GCM2, are essential for the survival of the thymus and parathyroid, respectively, and serve as early markers of each organ. However, these transcription factors are not the specifiers of the thymus or PT, and the specifiers remain unknown. An additional unknown mechanism of thymus and PT cell fate specification is the signals driving each fate from the surrounding mesenchyme, pharyngeal endoderm, and surface ectoderm. To identify candidate transcription factors specifying the thymus and PT, as well as extracellular signals driving such specifiers, I performed scRNA-seq on the 3rd PP and its surrounding tissues at two timepoints spanning thymus and parathyroid cell fate specification (E10.25-11.25). Using these data, I identified *Vgll2* and *Sox2* as candidate genes acting cell autonomously to control 3rd PP cell fates. I also identified *Wnt4/6* as a candidate signal driving the thymus cell fate, with the WNT inhibitor, *Sfpr2* as a

candidate permissive signal for the parathyroid cell fate. A second part of my project is to characterize the cell cycle gating of the SHH response. Using the FUCCI cell cycle reporter system, I show that cells in G2/M phases of the cell cycle are able to respond to SHH at a higher frequency. This study provides new information into how the thymus and parathyroid cell fates are specified, and how cells are able to perceive their environment throughout the cell cycle.

INDEX WORDS: Thymus, parathyroid, third pharyngeal pouch, scRNA-seq, Foxn1, Gcm2, Vgll2, Sox2, Shh, Wnt, Bmp, development, signaling, cell fate specification

IDENTIFYING MECHANISMS OF THYMUS AND PARATHYROID CELL FATE SPECIFICATION

by

MICHAEL NUNNELEY

BS, Eckerd College, 2012

MS, Georgia State University, 2016

A Dissertation Submitted to the Graduate Faculty of The University of Georgia in Partial Fulfillment of the Requirements for the Degree

DOCTOR OF PHILOSOPHY

ATHENS, GEORGIA

2023

IDENTIFYING MECHANISMS OF THYMUS AND PARATHYROID CELL FATE SPECIFICATION

by

MICHAEL NUNNELEY

Major Professor:	Nancy Manley
	Jonathan Eggenschwiler
Committee:	James Lauderdale
	Doug Menke
	Mike White

Electronic Version Approved:

Ron Walcott
Vice Provost for Graduate Education and Dean of the Graduate School
The University of Georgia
May 2023

ACKNOWLEDGEMENTS

First, I would like to thank my advisors, Jonathan Eggenschwiler, and Nancy Manley for encouraging me to pursue this difficult project. They have been great advisors, and always challenged me to find new ways to think about science. Without their help and support, I would not have gained the skills and knowledge that I did during this project. I would also like to thank my committee, Jim Lauderdale, Doug Menke, and Mike White for giving me advice and guidance during my committee meetings and our group developmental biology meetings. I would also like to thank all of the current and past members of the Eggenschwiler and Manley labs who helped me in lab meetings. Finally, I would like to thank all my incredible friends and family that have supported me throughout this experience. This project would not have been possible without their support outside of the lab.

TABLE OF CONTENTS

Page

LIST OF TABLES

Page

LIST OF FIGURES

Page

CHAPTER 1

GENERAL INTRODUCTION

Thymus and Parathyroid overview and function

Two vital organs, the thymus and the parathyroid, share one thing in common: their origin in the developing embryo. The thymus is responsible for T cell maturation in the adult, which is essential for adaptive immunity, while the parathyroid expresses parathyroid hormone to control extracellular calcium levels. However, despite their difference in function, both organs arise from a common primordium: the third pharyngeal pouch endoderm.

The function of the thymus remained unknown until the 1960s, when it was surgically removed from newborn mice and shown that they were unable to reject skin grafts, suggesting it had a role in self recognition of immune cells (Miller, 1965). Lymphocytes were also shown to accumulate in the thymus, and thymectomy resulted in reduced antigen reactive cells, but not reduce progenitor cells, suggesting the thymus is responsible for maturing T cells (Miller & Mitchell, 1967). Additional evidence of the role of the thymus came from the immunocompromised “nude” mice that lack hair, and more importantly, a thymus in the adult mouse (Pantelouris, 1968).

The primary functional component of the thymus are thymic epithelial cells (TECs). Thymic epithelial cells can be broadly characterized by their location in either the cortex (cTECs) or the medulla (mTECs). Immature T cell precursors enter the thymus through blood vessels at the border of the medulla and cortex, and travel through the

medulla and cortex as they mature before exiting the thymus back into the blood stream (Lind et al., 2001). The parathyroids produces parathyroid hormone (PTH) to regulate extracellular calcium levels and are located in the neck, next to the thyroid. The parathyroids respond to low levels of serum calcium levels by releasing PTH, which leads to increased reabsorption of calcium in the kidneys and release of calcium from osteoclasts in bone. Understanding how the functionally distinct thymus and the parathyroids arise from a common primordium has been the focus of much research over the last several decades as it poses an intriguing developmental biology question and could lead to therapies for individuals with impairments in thymus or parathyroid function.

Thymus and Parathyroid development timeline and migration

Although the thymus and the parathyroid have different functions and reside in different locations of the adult body, they share a common primordium: the third pharyngeal pouch (3rd PP). The 3rd PP is an outgrowth of the pharyngeal endoderm that begins to grow towards the surface ectoderm around E9. The surface ectoderm and ventral region of the third pharyngeal pouch make contact by E10, and stay connected until around E11, when migrating neural crest cells inhabit the space between the 3rd PP and surface ectoderm (Cordier & Heremans, 1975). The dorsal region of the 3rd PP gives rise to the parathyroid, while the ventral region gives rise to the thymus. Originally, it was hypothesized that the thymus was derived from both 3rd PP endoderm and surface ectoderm. This assumption was based off the physical contact of the surface ectoderm and presumptive thymus domain of the 3rd PP, as well as the "nude" mouse model that

both lacked a thymus and had skin defects (Cordier & Haumont, 1980; Cordier & Heremans, 1975). However, dye based lineage tracing and pharyngeal endoderm explant experiments showed that the thymus does not have any ectodermal contribution (Gordon et al., 2004). The pharyngeal endoderm explants were, however, cultured under the kidney capsule, which likely sends inductive signals. It is therefore possible that although the thymus does not have an ectodermal lineage, it may receive signals from the surface ectoderm during its development.

By E12.5, the thymus and parathyroid domains separate from the ectoderm and pharyngeal endoderm, and begin to migrate towards their final locations. This migration is likely mediated by the surrounding neural crest cells as the failure of NCCs to migrate to the pharyngeal region in *Pax3* Splotch mutants results in impaired migration (Griffith et al., 2009). Similarly, conditional deletion of *EphrinB* from NCCs results in impaired thymus migration (Foster et al., 2010). Migration of the parathyroid is likely mediated by its attachment to the thymus, as it does not appear to migrate after its separation from the thymus between E12.5-E13.

Two key transcription factors in thymus/parathyroid differentiation

Thymus and parathyroid primordia can be identified early in organogenesis by the differential expression of two key transcription factors in the 3rd PP: *Gcm2* and *Foxn1* (Gordon et al., 2001). These two genes are key for organ survival and function. *Gcm2*$^{-/-}$ mice fail to form a functioning parathyroid as the parathyroid primordium fails to produce PTH and fails to maintain other parathyroid specific markers, and subsequently undergoes apoptosis (Günther et al., 2000; Liu et al., 2007). *Foxn1* is the gene mutated in

nude mice (Kaestner et al., 2000; Segre et al., 1995). The thymus domain in *Foxn1-/-* mice initially develops but does not become a functioning thymus (Nehls et al., 1996). Because the thymus and parathyroid primordium are formed in *Foxn1* and *Gcm2* mutants respectively, these genes are not the specifiers of each organ.

The specification process of the thymus and parathyroid happens over a short period of time. Around E10, *Gcm2* is expressed in the dorsal-anterior region of the 3rd PP and marks the presumptive parathyroid domain. By E11, *Foxn1* is expressed in the ventral region of the 3rd PP marking the presumptive thymus domain, while the central region of the 3rd PP remains *Gcm2/Foxn1* negative (Gordon et al., 2001; Griffith et al., 2009). By E11.5 the entire 3rd PP is marked by *Gcm2* in the dorsal parathyroid domain, and *Foxn1* in the ventral thymus domain (Figure 1.1).

Transcription factors studied in thymus/parathyroid specification

Although *Foxn1* and *Gcm2* are early makers of the thymus and parathyroid and necessary for organ function and differentiation, they are not the specifiers of each organ. The roles of several other genes in thymus and parathyroid specification have been investigated. The transcription factor, *Tbx1*, has long been a focus of researchers due to its role in causing DiGeorge syndrome, a disease with multiple symptoms including facial defects, parathyroid defects, and immune deficiencies (Jerome & Papaioannou, 2001; Merscher et al., 2001; Yagi et al., 2003). *Tbx1* is expressed throughout the 3rd PP at E9.5, as well as the surrounding mesenchyme, but is restricted to the mesenchyme and dorsal region of the 3rd PP by E10.5 (F. Vitelli et al., 2002). *Tbx1*$^{-/-}$ mice have both thymus and parathyroid hypoplasia (Jerome & Papaioannou, 2001). Interpreting the role

of *Tbx1* in thymus or parathyroid cell fate specification based on these results is difficult as the pharyngeal pouches fail to form in *Tbx1* mutants (Arnold et al., 2006; Lindsay et al., 2001; Francesca Vitelli et al., 2002). However, ectopic expression of *Tbx1* throughout the 3rd PP restricts *Foxn1* expression to the most ventral region of the 3rd PP, suggesting that *Tbx1* inhibits *Foxn1*. Although *Foxn1* is restricted when *Tbx1* is overexpressed, the central region of the 3rd PP remains *Gcm2/Foxn1* negative, suggesting that *Tbx1* also does not specify the parathyroid cell fate (Reeh et al., 2014). Another transcription factor, *Foxi3*, interacts with *Tbx1* and is also necessary for proper pharyngeal pouch outgrowth, but is unlikely to be involved in cell fate specification of the thymus or parathyroid (Hasten & Morrow, 2019).

Another transcription factor that plays a role in 3rd PP cell fate specification is *Hoxa3,* which is has an anterior expression limit at the 3rd pharyngeal arch and is expressed throughout the 3rd PP and its surrounding tissues (Chisaka & Capecchi, 1991; Gaunt, 1987, 1988; Manley & Capecchi, 1995). Initial studies into the role of *Hox3* paralogs in thymus and parathyroid development showed that *Hoxa3^{null}* mutants initially form pharyngeal pouches but lack thymus and parathyroids. Other *Hox3* paralogs do not play a major role in thymus/parathyroid organogenesis as *Hoxa3+/-/Hoxb3-/-;Hoxd3-/-* mutants have ectopically located thymus and parathyroids (Chisaka & Capecchi, 1991; Manley & Capecchi, 1995). Interestingly, a closer look at the 3rd PP over the timeline of thymus and parathyroid specification shows that *Gcm2* and *Foxn1* are transiently expressed in *Hoxa3$^{-/-}$* mutants. However, *Gcm2* expression is lost by E11.5, while *Foxn1* expression is initiated at E12, about a day later than wild-type animals, and the thymus is undetected by E13.5 (Chojnowski et al., 2014). *Hoxa3* is also necessary for the

expression of *Bmp4* and *Fgf8* in the ventral region of the 3rd PP (Chojnowski et al., 2014). Because *Hoxa3* mutants exbibit defects in both thymus and parathyroids, yet both organs are present for short periods, it is likely that it is necessary for the 3rd PP identity in general, but does not specify the thymus or parathyroid cell fates individually.

Hoxa3 is implicated to be in a *Hoxa3-Pax1/9-Eya1-Six1/4* regulatory network necessary for 3rd PP cell fates. The PAX/SIX/EYA gene regulatory network was discovered in regulating drosophila eye development, but has been well described across other tissues and other organisms (Fortunato et al., 2014). In the mouse 3rd PP, this network is necessary for proper pouch development, but like *Hoxa3*, does not regulate the thymus or parathyroid cell fate individually. While $Pax1^{-/-}$ mutants have reduced parathyroid and thymus, $Hoxa3^{+/-};Pax1^{-/-}$ mutants are more severe, with reduced or absent *Gcm2* and parathyroids (Su et al., 2001; Wallin et al., 1996). $Pax9^{-/-}$ mutant mice have a more severe phenotype than $Pax1^{-/-,}$ and lack both thymus and parathyroids (Peters et al., 1998). While $Six1^{-/-}$ mice have reduced *Gcm2* and *Foxn1*, $Six1^{-/-};Six4^{-/-}$ double mutants have absent *Gcm2* and *Foxn1* expression. *Eya1* is likely upstream of *Six1*, as $Eya1^{-/-}$ mutant mice lack thymus, parathyroid, and *Six1* expression in the 3rd PP (Xu et al., 2002; Zou et al., 2006). The function of *Eya1* in the 3rd PP is likely not carried out completely by *Six1*, however, as *Eya1-/-* mutant mice also lack *Tbx1* and *Fgf8* expression, a phenotype not observed in $Six1^{-/-}$ mice. *Pax1*, but maybe not *Pax9*, is downstream of *Eya1/Six1*, as $Eya1^{-/-};Six1^{-/-}$ mice fail to express *Pax1* (Zou et al., 2006). Overall, the PAX/SIX/EYA gene regulatory network is necessary for proper 3rd PP development but does not specify either the thymus or parathyroid cell fates individually as both organs are affected in such mutants.

While *Hoxa3, Pax1/9, Eya1, Six1, Tbx1,* and *Foxi3* have been shown to affect 3rd PP development, all are expressed throughout the 3rd PP at early stages, and mutants do not affect only the thymus or parathyroid individually (Peters et al., 1998; Su et al., 2001; Wallin et al., 1996; Xu et al., 2002; Zou et al., 2006). In order to identify candidate cell fate specifiers of the thymus and parathyroid, a previous study took a literature based approach to identify transcription factors that are differentially expressed in the developing third pharyngeal pouch as candidate specifiers of the thymus or parathyroid cell fate (Wei & Condie, 2011). These transcription factors included *Foxg1, Isl1, Nkx2-5, Nkx2-6, Gata3,* and *Sox2.*

At E9.5, *Nkx2-5* is localized to the ventral region of the 3rd PP and is further restricted to the ventral tip of the 3rd PP at E10.5. *Nkx2-6* on the other hand, is broadly expressed throughout the 3rd PP at E9.5, and only loses expression in the dorsal third of the 3rd PP at E10.5. By E11.5, neither *Nkx2-5* or *Nkx2-6* are expressed in the 3rd PP. The expression of *Nkx2*-5 and *Nkx2-6* expression in the ventral region of the pouch, in proximity to *Bmp4* from the surface ectoderm and ventral neural crest mesenchyme, is consistent with the fact that BMPs drive *Nkx2-5* in other tissues (Jamali et al., 2001). Neither *Nkx2-5* or *Nkx2-6* mutants individually affect thymus or parathyroid development (Lyons et al., 1995; Tanaka et al., 1999; Tanaka et al., 2000). This is complicated by the fact that *Nkx2-5* and *Nkx2-6* may compensate for each other, as *Nkx2-5* expression is expanded in a *Nkx2-6* mutant. Identifying the role of *Nkx2-5* or *Nkx2-6* in thymus or parathyroid cell fate specification is further complicated as *Nkx2-5*$^{-/-}$*;Nkx2-6*$^{-/-}$ double mutant mice have defects in pharynx development well before thymus or parathyroid cell fate specification (Tanaka et al., 2001).

Three other transcription factors were shown through *in situ* hybridization on whole mount or sectioned embryos to be expressed in the presumptive thymus domain prior to *Foxn1* expression: *Foxg1, Gata3,* and *Isl1* (Wei & Condie, 2011). The transcription factor, *Foxg1*, has been studied in its role in brain development, as humans with haploinsufficiency in *Foxg1* have a range of neurological disorders (Hou et al., 2020). *Foxg1* is not detected in the 3rd PP at E9.5, prior to *Gcm2* and *Foxn1* expression. However, it is expressed in two domains of the pouch at E10.5: the ventral tip and the dorsal, anterior region of the pouch, which does not overlap with *Gcm2* at this stage. By E11.5, *Foxg1* is restricted to the thymus domain of the 3rd PP. Also, *Foxg1* null mutants do have both thymus and parathyroids, although later thymus development and TEC differentiation are affected (Wei and Condie, unpublished).

Gata3 has an interesting expression pattern over the timeline of specification. At E10.5, prior to *Foxn1* expression, *Gata3* is expressed in the presumptive thymus domain, in the ventral region of the 3rd PP. However, at E11.5, *Gata3* is no longer expressed in the ventral region of the 3rd PP, and instead is expressed in the dorsal parathyroid domain, about a day and a half after *Gcm2* expression is initiated (Wei & Condie, 2011). Humans with *Gata3* mutations have DiGeorge-like symptoms, similar to those caused by *Tbx1* mutations, that includes hypoparathyroidism and immune deficiencies (Van Esch et al., 2000). While in mice, *Gata3* has been shown to bind to the *Gcm2* promotor, the expression of *Gata3* beginning after initial *Gcm2* expression makes it more likely to maintain *Gcm2* expression rather than initiate it (Grigorieva et al., 2010). Additionally, *Gata3*$^{-/-}$ mice lack a thymus/parathyroid primordia by E12.5 (Grigorieva et al., 2010).

This phenotype, along with the temporal-spatial expression pattern of *Gata3* does not make it a strong candidate as a cell fate specifier of either the thymus or parathyroid.

Isl1 was shown to be expressed in the ventral region of the 3rd PP and the surface ectoderm from E9.5 through E11.5. The role of *Isl1* has been described in other tissues and plays a role in regulating the expression of several developmental signals. In the heart, *Is1* marks a set of progenitor cells. Mice with *Isl1* mutations lack an outflow tract, right ventricle, and part of the atria, and have decreased expression of BMPs and FGFs (Cai et al., 2003). In the limb bud, *Isl1* has been shown to regulate *Fgf10,* and in the developing genital tubercle, *Fgf10, Bmp4, and Wnt5a,* and in their absence the hind limb bud fails to form (Ching et al., 2018; Narkis et al., 2012). *Isl1* has also been implicated in mediating the Wnt/ß-catenin pathway in the limb-bud, as it facilitates the nuclear localization of ß-catenin (Kawakami et al., 2011).

The only transcription factor identified by Wei and Condie to be specific to the dorsal region of the 3rd PP during parathyroid cell fate specification was *Sox2* (Wei & Condie, 2011). *Sox2* is a well-studied transcription factor as it was identified as a Yamanaka factor, with its ability to induce pluripotent stem cells from fibroblasts along with *Oct3/4, Klf4,* and *c-Myc* (Takahashi & Yamanaka, 2006). In embryonic stem cells, *Sox2* has been shown through ChIP with DNA microarray to bind to DNA near multiple transcription factors, suggesting it plays a large role in pluripotency and cell fate specification (Boyer et al., 2005). At E9.5, *Sox2* was not detected in the 3rd PP by whole mount *in situ* hybridization. However, at E10.5, *Sox2* was expressed in the dorsal, posterior region of the 3rd PP. This expression pattern was hypothesized to partially overlap with *Gcm2* expression but was not proven as the *in situ* hybridizations were carried out with only

single probes (Wei & Condie, 2011). The proximity of *Sox2* expression at E10.5 to the pharyngeal endoderm, which expresses *Shh*, is consistent with the fact that SHH has been shown to drive *Sox2* expression in developing taste buds (Castillo-Azofeifa et al., 2018). By E11.5, *Sox2* expression was not detected in the 3rd PP (Wei & Condie, 2011). The differential expression of *Sox2* across the timeline of parathyroid specification makes it a good candidate for regulation of parathyroid cell fate specification.

Signaling pathways studied in thymus/PT specification.

Several signaling pathways have been identified as having a role in thymus and parathyroid specification, including SHH, BMPs, FGFs and WNTs. Two morphogens, *Shh* and *Bmp4* are expressed on opposite poles of the developing 3rd PP, and drive *Gcm2* and *Foxn1* respectively.

In the 3rd PP, *Shh* drives *Gcm2* expression. *Shh* is expressed in the adjacent pharyngeal endoderm starting at E9.5, and continues to be expressed through E11.5, as the 3rd PP begins to separate from the pharyngeal endoderm. The SHH receptor, *Ptch1*, often a readout of cells responding to SHH, is expressed in the dorsal region of the 3rd PP and the mesenchyme close to the pharyngeal endoderm, suggesting that both dorsal 3rd PP endodermal cells and the dorsal mesenchyme responds to SHH from the pharyngeal endoderm (Moore-Scott & Manley, 2005). In a $Shh^{-/-}$ mutant, the third pharyngeal pouch forms and expresses 3rd PP identity markers such as *Hoxa3, Fgf8,* and *Pax1*, although it does have altered morphology with increased cell death and decreased proliferation. Although the 3rd PP forms, *Gcm2* is not detected by whole mount *in situ* hybridization in

a *Shh*$^{-/-}$ mutant, and *Foxn1* is expressed throughout the pouch (Moore-Scott & Manley, 2005).

As a *Shh* null mutant fails to express *Gcm2*, one would expect that blocking the SHH signal response specifically in the 3rd PP endoderm would result in a similar phenotype. However, conditional activation or repression of the SHH signal response in the 3rd PP endoderm or surrounding NCC mesenchyme have unexpected results on *Gmc2* and *Foxn1* expression patterns. When the SHH signaling effector, *Smoothened (Smo)*, is conditionally deleted in the endoderm using *Foxa2-Cre*^{ER}, *Gcm2* is expressed, as opposed to the lack of expression seen in a *Shh*$^{-/-}$ null mutant. However, conditional disruption of *Smo* in the endoderm does result in an ectopic *Foxn1* positive domain in the dorsal region of the 3rd PP. On the other hand, 3rd PP cells can be forced to activate the SHH pathway regardless of their distance to the SHH source using a conditionally active *Smo* allele: *R26iSmoM2*. In *Foxa2-CreER;R26iSmoM2* embryos, *Foxn1* expression is lost in the central region as expected. However, *Gcm2* expression does not expand into the central region of the pouch, and *Foxn1* expression is maintained in the ventral region of the pouch, leaving a dorsal *Gcm2* positive domain, a ventral *Foxn1* domain, and a central domain that is negative for both *Gcm2* and *Foxn1* well after WT embryos express *Gcm2* or *Foxn1* throughout the 3rd PP. The loss of *Foxn1* expression in the central domain of the 3rd PP in this model is likely due to the observed expansion of the PT specific *Foxn1* inhibitor, *Tbx1* (Bain et al., 2016). However, two major questions remain unanswered from the results observed in *Foxa2-CreER;R26iSmoM2* embryos: how are the ventral cells still able to express *Foxn1,* and why do the central cells which are *Foxn1* negative and *Tbx1* positive fail to express *Gcm2.*

Similar to altering the SHH response in the 3rd PP, activating or inhibiting the SHH pathway activity specifically in the surrounding NCC mesenchyme also affects *Gcm2* and *Foxn1* expression. A conditional knockout of *Smo* from the NCC mesenchyme using *Wnt1-Cre* results in a disordered central region of the 3rd PP, with *Foxn1* positive and *Gcm2* positive cells being intermingled without a defined *Foxn1-Gcm2* border as seen in WT embryos. On the other hand, activating the SHH pathway in NCC mesenchyme in *Wnt1-Cre;R26iSmoM2* embryos causes a loss of *Gcm2* and *Foxn1* positive cells in the central region of the 3rd PP (Bain et al., 2016). Taken together, these results suggest that the NCC mesenchyme expresses a signal that drives *Gcm2* and *Foxn1* in the central region of the 3rd PP, and production of this signal by NCCs is dependent on their ability to properly respond to SHH.

Although SHH is the only known signal to be specifically required for *Gcm2* expression, several other signals are known to control *Foxn1* expression. While *Shh* is expressed in the pharynx, adjacent to the parathyroid domain, *Bmp4* is expressed in the ventral NCC mesenchyme, ventral 3rd PP cells, and the surface ectoderm starting between E9.5 and E10.5, prior to *Foxn1* expression. The BMP inhibitor, *Noggin*, is expressed in the parathyroid domain at E10.5-E11.5, suggesting that BMPs drive the thymus fate, while the parathyroid must inhibit BMP signaling (Patel et al., 2006). However, functional tests of the role of BMP signaling in thymus cell fate specification have proved to be complicated. While a deletion of *Bmp4* from the 3rd PP and surrounding mesenchyme in *Foxg1-Cre;Bmp4* embryos caused defects in thymus migration and mesenchyme condensation around the thymus, it did not cause a loss of *Foxn1* expression (Gordon et al., 2010). However, this result is complicated by the fact that *Bmp4* was not

deleted from the surface ectoderm, which contacts the 3rd PP shortly before *Foxn1* expression is initiated. Similarly, other BMPs could be expressed in the region that may compensate for the loss of *Bmp4.*

Other evidence that BMPs drive *Foxn1* come from thymic organ culture, where thymic cells cultured with BMP4 have increased *Foxn1* expression (Tsai et al., 2003). However, mechanisms regulating *Foxn1* expression in the mature thymus may differ from those regulating initial thymus cell fate specification. The most convincing evidence that BMPs regulate thymus cell fate comes from the chick, where pharyngeal pouch explants cultured on mesenchyme cells that presumably express BMPs express *Foxn1* but fail to express *Foxn1* with the addition of Noggin (Neves et al., 2012). Noggin is expressed in the dorsal region of the 3rd PP, suggesting it may inhibit a BMP response in the presumptive thymus (Patel et al., 2006). Taken together, it is likely that an opposing gradient of SHH and BMPs help drive thymus and parathyroid cell specification, additional signals also play a role in for 3rd PP cell fate specification.

In addition to BMPs, FGFs have also been studied in their roles in thymus cell fate specification. *Fgf8, Fgf3,* and *Fgf15* are early markers of the ventral domain of the 3rd PP, being expressed in the ventral 3rd PP at E10.5, prior to *Foxn1* expression (Gardiner et al., 2012). However, genetically testing the function of FGFs in thymus and parathyroid specification is not easy due to multiple functions of FGFs and the potential for compensation among individual FGF signals. The FGF pathway inhibitors *Spry1* and *Spry2* are co-expressed with FGFs in the 3rd PP. While a *Spry1/2* dKO embryos show an increase in FGF signaling response in the 3rd PP as evidenced by increased *Etv5* and *Dusp6* expression, they did not exhibit a change in *Gcm2* or *Foxn1* expression (Gardiner et al.,

2012).

Another signaling pathway implicated in thymus development are WNTs. However, studies investigating WNT signaling in thymus development have largely focused on the thymus organ post-specification. In one study, over-expression of *Wnt4* using *Foxn1::Wnt4* transgenic mice showed that increased WNT signaling caused defects in thymus function and migration (Swann et al., 2017). It is important to note, however, that the over expression of *Wnt4* in this experiment occurs after thymus cell fate specification, and the mature thymus in wildtype mice expresses several Wnts including *Wnt4* (Pongracz et al., 2003).

More convincing evidence of WNTs playing a role in thymus development comes from thymic epithelial cell culture. Cultured thymic epithelial cells with stimulated WNT signaling using either WNT4 or LiCl showed an increase in *Foxn1* expression. Furthermore, *Foxn1* expression induced by LiCl did not decrease in the presence of Cycloheximide, suggesting the WNT signaling pathway directly regulates *Foxn1* in thymic epithelial cells (Balciunaite et al., 2002). However, this study was also performed in already specified thymus cells, and an earlier role of WNTs in specifying 3rd PP cell fates has not been investigated.

There is also evidence of a third signal from the NCC mesenchyme specifying third pharyngeal pouch cell fates. The most convincing evidence of the NCC mesenchyme signaling to the third pharyngeal pouch comes from the *Pax3*$^{sp/sp}$ mutant, in which neural crest cells fail to migrate to the pharyngeal arches. In *Pax3*$^{sp/sp}$ mutants, the *Gcm2-Foxn1* border in the central region of the 3rd PP shifts so that there is an increase in *Foxn1* and a decrease in *Gcm2* expression (Griffith et al., 2009). As mentioned previously, this signal

may be driven by SHH, as alterations in the SHH response specifically in the NCC mesenchyme results in changes to *Foxn1* and *Gcm2* expression in the central region of the 3rd PP (Bain et al., 2016). It is important to note, however, that these phenotypes are apparent in the central region of the pouch, but *Foxn1* and *Gcm2* are still initiated in the dorsal and ventral regions. Therefore, the initial specification of the thymus and parathyroid identities do not depend on signals from the NCC mesenchyme. The extracellular signals driving initial thymus and parathyroid fates likely come from the pharyngeal endoderm, contacting the presumptive parathyroid domain, and the surface ectoderm, which transiently contacts the presumptive thymus domain. However, such signals remain unidentified.

Sonic Hedgehog signaling pathway

Sonic hedgehog is necessary for parathyroid cell fate specification but is also involved in many developmental processes including patterning in multiple tissues, regulating cell cycle dynamics, and has a non-canonical function in axon guidance. The mechanism of transduction of SHH signals is complicated and still not fully understood. Through a cascade of protein-protein interaction and modification, the canonical response to SHH is ultimately carried out by the GLI transcription factors, which can act as both an activator and inhibitor of the pathway. There are three mammalian Gli proteins: GLI1, GLI2, and GLI3. *Gli1* is transcribed in response to SHH pathway activation, and acts as an activator of the pathway's transcriptional response (i Altaba et al., 2007; Katoh & Katoh, 2009). GLI2 and GLI3 are present in cells, but act as repressors in the absence of SHH signaling and undergo post-transcriptional modifications to act as activators in the

presence of SHH (Altaba, 1999; Sasaki et al., 1999). In the absence of SHH, GLI transcription factors are truncated into an N-terminus repressor form, while in the presence of SHH they remain in a full-length activator form (Niewiadomski et al., 2014; Wang & Li, 2006).

SHH initially binds to its transmembrane receptor, *Patched* (*Ptch1*). In the absence of the SHH ligand, PTCH1 is an inhibitor of the pathway, inhibiting the transmembrane protein and SHH pathway activator, *Smoothened (Smo)*, from entering the cilia (Taipale et al., 2002). In the presence of SHH, PTCH1 is inhibited, which removes the inhibition of SMO and allows SMO to enter the cilia and accumulate at the tip of the cilia (Milenkovic et al., 2015; Rohatgi et al., 2007; Torroja et al., 2004).

In the absence of SHH, the GPCR, GPR161, accumulates in the cilia and increases cyclic AMP levels, which in turn increases PKA activation (Bishop et al., 2007). PKA represses the SHH response in the absence of SHH by phosphorylating GLI2 and GLI3 (Kotani, 2012; Niewiadomski et al., 2014). PKA also acts with GSK3- β to phosphorylate and stabilizes the SHH repressor, SUFU (Chen et al., 2011). In the absence of SHH, SUFU binds to GLIs and prevents their localization to the nucleus (Priit Kogerman et al., 1999; Svärd et al., 2006).

Cell cycle overview

SHH signaling is known to affect the cell cycle in part by upregulating the expression of *cyclinD1/cyclinD2* (Kenney & Rowitch, 2000). The cell cycle is controlled by the temporal expression of cyclins which interact with cyclin dependent kinases (CDKs) to phosphorylate target proteins and progress cells through gap 1 (G1), S, G2,

and mitosis phases. Cells in the G1 phase of the cell cycle express D type cyclins (*cyclinD1, cyclinD2, cyclinD3*), which interact with CDK4/6 (Sherr, 1994). The CyclinD/CDK4/6 complex phosphorylates RB, which removes its inhibition on the E2F transcription factor (Brehm et al., 1998; Buchkovich et al., 1989; Kato et al., 1993). This leads to the upregulation of cyclinE (*cyclinE1, cyclinE2*), which interacts with CDK2 leading to the initiation of S phase (Ohtani et al., 1995; Ohtsubo et al., 1995). During S phase, cyclinA(*cyclinA1/cyclinA2*)/CDK2 are necessary to initiate DNA replication by phosphorylating DNA polymerase alpha primase and to inhibit E2F activity in a negative feedback loop (Girard et al., 1991; Voitenleitner et al., 1997; Xu et al., 1994). CyclinA also acts with CDK1 to promote the entry into mitosis (King et al., 1994).

Cell cycle effects on cell fate

The cell cycle has been shown in several contexts to influence cell fate. In WNT signaling, cells are more responsive to WNTs in the G2/M phases of the cell cycle. The G2 cell phase specific cyclin, cyclinY/CDK14, phosphorylates the WNT receptor, LRP6. This phosphorylation makes the LRP6 receptor most active during G2 (Davidson et al., 2009). Furthermore, a *cyclinY* morphant downregulated a WNT response reporter and caused anteriorization in *Xenopus* as would be expected with a loss of WNT activity (Davidson et al., 2009). Supporting the increased WNT response in G2, another study demonstrated that the WNT response effector, β-Catenin, accumulates during the cell cycle and is highest in G2 (Olmeda et al., 2003).

Another example of the cell cycle affecting the cells ability to respond to signals comes from embryonic stem cells that have a higher Activin pathway response in the

early G1 phase of the cell cycle. Cyclin Ds activate CDK4/6, which phosphorylates the Activin signaling transducers, SMAD2/3 in late G1 and prevent their nuclear localization. (Pauklin & Vallier, 2013). Cyclin Ds also play a role in cell fate specification independent of CDK4/6 activation as they are able to recruit co-repressors and co-activators to endoderm, mesoderm, and neuroectoderm genes in human pluripotent stem cells (Pauklin et al., 2016).

In the thymus, E2F has been shown to directly regulate *Foxn1* expression. Mice with a conditional knockout of RB family proteins from the thymus that have increased E2F activity also have an increase in *Foxn1* expression. Additionally, E2F is shown to bind directly to two sites in the *Foxn1* promotor. However, this phenotype was only observed in mice three months and older, suggesting E2F plays a role in the aging thymus, but does not drive *Foxn1* in early stages (Garfin et al., 2013).

This study aims to identify mechanisms of thymus and parathyroid cell fate specification and address of cell cycle gating of SHH responses. To identify mechanisms of cell fate specification of the thymus and parathyroid, we used scRNA-seq to identify differentially expressed transcription factors and extracellular signals over the timeline of specification. We then used fluorescent *in situ* hybridization to confirm expression patterns and strengthen or weaken hypotheses generated from the scRNA-seq data. To determine whether and how the Hedgehog pathway is gated by cell cycle phase, we used the cell cycle phase reporter, FUCCI, to monitor the activity of the Hedgehog pathway activation of *Gli1* nascent mRNA expression across different phases of the cell cycle. This data showed that cells in the G2/M phase of the cell cycle respond to SHH at a higher frequency than cells in other phases of the cell cycle.

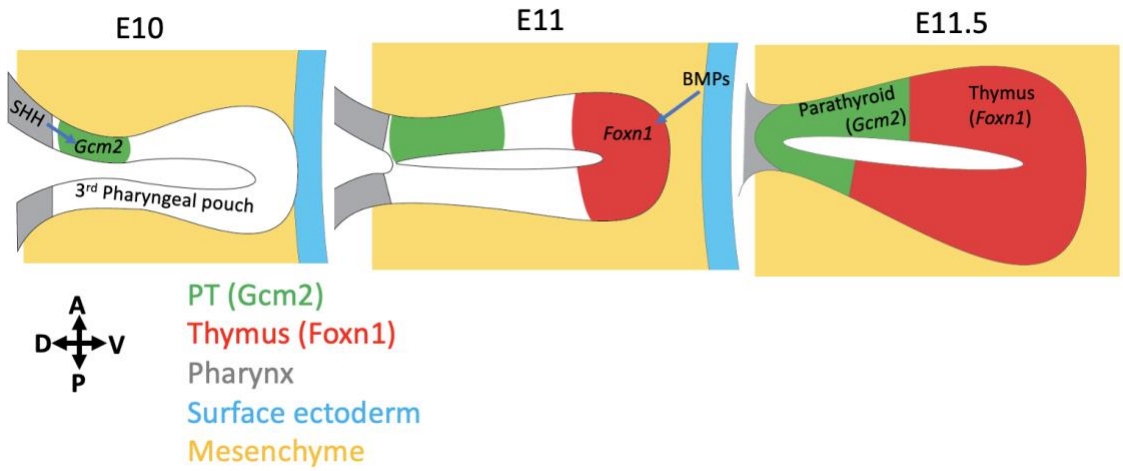

Figure 1.1. Third pharyngeal pouch patterning and development. The 3rd PP begins to grow out of the pharyngeal endoderm at E9.5. At E10, SHH from the pharynx drives *Gcm2* in the dorsal parathyroid domain. At E11, BMPs from the ventral mesenchyme, ectoderm, and ventral 3rd PP drive *Foxn1* in the thymus domain. The central region remains marker negative until E11.5, when the entire 3rd PP is marked by *Gcm2* and *Foxn1*.

CHAPTER 2

IDENTIFYING MECHANISMS OF THYMUS AND PARATHYROID CELL FATE SPECIFICATION USING SINGLE CELL RNA-SEQ

Introduction

Two essential organs, the thymus and the parathyroid, have far different functions in the adult organ and are in different locations in the adult, but share a common primordium. The question as to how some cells in this primordium are specified into the thymus fate, while others are specified into the parathyroid fate has remained unanswered. This study aims to identify mechanisms of thymus and parathyroid cell fate specification using a single cell RNA-seq approach.

Both the thymus and the parathyroid arise from the third pharyngeal pouch (3rd PP), an outgrowth of the pharyngeal endoderm in the mouse embryo. Two transcription factors, *Foxn1* and *Gcm2*, are early markers of the thymus and parathyroid cell fate, respectively, and are necessary for downstream survival and function of each organ, but do not specify either organ (Gordon et al., 2001; Liu et al., 2007; Nehls et al., 1996). The 3rd PP begins to grow out of the pharyngeal endoderm at E9 until it contacts the surface ectoderm around E10, a process dependent on the transcription factor, *Tbx1* (Hasten & Morrow, 2019). At E10, the transcription factor, *Gcm2*, begins to be expressed in the dorsal, anterior region of the 3rd PP, marking the parathyroid domain (Gordon et al., 2001). At E11 the expression of *Foxn1* is initiated in the ventral tip of the 3rd PP, but the central region remains marker negative. Over the next half a day, the central region of the

3rd PP gradually expresses *Foxn1* and *Gcm2*, until the entire 3rd PP is marked by *Gcm2* in the dorsal parathyroid domain and *Foxn1* in the ventral thymus domain (Bain et al., 2016; Gordon et al., 2001). While several transcription factors are necessary for both thymus and parathyroid cell fates, none have been shown to drive either the thymus or parathyroid individually (Peters et al., 1998; Su et al., 2001; Wallin et al., 1996; Xu et al., 2002; Zou et al., 2006). The transcription factors specifying the thymus or parathyroid cell fates that would be upstream of *Gcm2* and *Foxn1* have yet to be identified.

The third pharyngeal pouch is surrounded by a variety of tissues, including neural crest cell (NCC) derived mesenchyme, the pharyngeal endoderm, which contacts the dorsal parathyroid domain, and the surface ectoderm, which transiently contacts the ventral thymus domain at E10. Several extracellular signals are expressed in these surrounding tissues and have been implicated in thymus and parathyroid cell fate specification, but none have been shown to be the sole drivers of either cell fate (Bain et al., 2016; Gardiner et al., 2012; Gordon et al., 2010; Moore-Scott & Manley, 2005; Patel et al., 2006). *Shh* is expressed in the pharyngeal endoderm, adjacent to the parathyroid domain, and the ligand signals to both the dorsal pharyngeal pouch and the dorsal NCC mesenchyme, as evidenced by induction of *Ptch1* expression (Moore-Scott & Manley, 2005). SHH is necessary for the parathyroid identity, as *Shh* null embryos fail to express *Gcm2* (Moore-Scott & Manley, 2005). However, blocking the 3rd PP specifically from responding to SHH using an endoderm specific Cre to knockout *Smo* (*Foxa2-Cre^{ER};Smo*) fails to block *Gcm2* expression, but does lead to ectopic *Foxn1* expression in the dorsal domain (Bain et al., 2016). Additionally, SHH does not appear sufficient to drive *Gcm2* expression, as forcing a SHH pathway activity in the 3rd PP with a constitutively active

Smo allele (*Foxa2-CreER;R26iSmoM2*) reduces the domain of *Foxn1* expression, presumably due to the expanded expression of the *Foxn1* inhibitor, *Tbx1* (Bain et al., 2016; Reeh et al., 2014). Although the *Foxn1+* domain is reduced in *Foxa2-CreER;R26iSmoM2* and the *Tbx1+* domain expands, the *Gcm2+* domain does not expand and cells in the central region remain *Foxn1* and *Gcm2* negative (Bain et al., 2016).

Several signals have been implicated in driving the thymus cell fate, but there are no mutations in signaling factors showing a specific failure to induce *Foxn1* expression. *Bmp4* is expressed in the ventral NCC mesenchyme, the surface ectoderm, and the ventral 3rd PP at E10.5 (Patel et al., 2006). While explant studies in the chick have shown that the BMP inhibitor, *Noggin*, inhibits *Foxn1*, suggesting a role for BMPs in driving *Foxn1* expression, experiments in the mouse are difficult (Neves et al., 2012). Mice with a conditional knockout of *Bmp4* from the NCC mesenchyme and 3rd PP still express *Foxn1*, but this phenotype may be explained by compensation of other BMPs or the expression of *Bmp4* from the surface ectoderm (Gordon et al., 2010). WNTs have also been shown to drive *Foxn1* expression in differentiated thymic cells but their role have not been investigated in the embryo prior to thymus cell fate specification (Balciunaite et al., 2002).

An additional, unknown signal from the NCC mesenchyme is implicated in inhibiting the thymus cell fate in the central region of the 3rd PP. In mice that fail to migrate NCC mesenchyme to the pharyngeal arches (*Pax3*$^{splotch/splotch}$) there is an increase of *Foxn1* and a decrease of *Gcm2* expression in the central region of the 3rd PP (Griffith et al., 2009). This signal may be driven by SHH, as mice with forced SHH activity in the NCC mesenchyme (*Wnt1-Cre;R26iSmoM2*) lose expression of *Gcm2* and *Foxn2* in the

central region of the 3rd PP (Bain et al., 2016). The fact that *Foxn1* is expressed in the absence of NCC mesenchyme in *Pax3*$^{splotch/splotch}$ mice also suggests that the primary signaling center driving the thymus cell fate is not in the NCC mesenchyme and instead may be the surface ectoderm or the 3rd PP itself (Griffith et al., 2009).

The identification of thymus and parathyroid cell fate specifiers and inductive signals has been hindered by a lack of knowledge of the transcriptomes during specification events. The purpose of this project is to identify candidate cell-autonomous transcription factors specifying the thymus and parathyroid cell fates, as well as candidate signals from surrounding tissues driving expression of such specifiers. To do this, we took a single cell RNA-seq approach over the timeline of specification to identify differentially expressed transcription factors between the thymus and parathyroid domains, as well as differentially expressed extracellular signals in the surrounding tissues.

We performed scRNA-seq on the 3rd PP and surrounding tissues at E10.25 and E11.25. At E10.25, *Gcm2* expression has just been initiated, but the thymus domain is thought to have not been specified yet, as *Foxn1* expression is not initiated until E11 (Bain et al., 2016; Gordon et al., 2001). Ideally, this timepoint would allow us to identify transcription factors that are expressed in actively specifying parathyroid cells and transcription factors that are expressed in the presumptive thymus domain prior to *Foxn1* expression. At our second single cell RNA-seq timepoint, E11.25, the 3rd PP expresses *Gcm2* in the parathyroid region and *Foxn1* in the ventral thymus region but contains some *Foxn1* negative *Gcm2* negative cells in the central region. This would allow us to use known marker genes to identify thymus and parathyroid cells and identify

differentially expressed transcription factors between such cells. All scRNA-seq tissue collection also included tissues surrounding the 3rd PP, allowing us to identify differentially expressed signals from surrounding tissues that serve as candidate signals driving the thymus and parathyroid cell fates.

To support or rule out candidate genes identified from scRNA-seq experiments, we confirmed their expression patterns over the timeline of specification using fluorescent *in situ* hybridization. We further tested their expression patterns in a mouse model with known changes to *Foxn1* and *Gcm2* expression, the SmoM2 model described earlier (*Sox17-Cre;R26iSmoM2*). Because these SmoM2 embryos show a reduction of the *Foxn1+* domain, while the *Gcm2+* domain is not expanded, there is a region of *Gcm2* negative, *Foxn1* negative cells at E11.5. We can therefore observe candidate specifiers of the thymus and parathyroid in these mice to determine if such candidates mirror the expression of *Foxn1* or *Gcm2* as would be expected of a transcription factor driving either gene, or if they are expressed in the marker negative cells. We would not expect candidate drivers of either cell fate to be expressed in the marker negative cells and as the specifier of the thymus or parathyroid likely drives *Gcm2* or *Foxn1* respectively.

Methods

Single cell RNA-seq dissections

In order to maximize reads per cell in cells of interest, dissections were done in a way to minimize non-target cells. Cells targeted for dissections included 3rd pharyngeal pouch cells to identify candidate cell-autonomous regulators of thymus and parathyroid cell fate, as well as cells surrounding the third pharyngeal pouch to identify candidate

signals driving 3rd pharyngeal pouch cell fates. At E10.25, the 3rd pharyngeal pouch is visible under a dissecting microscope, and is a relatively large proportion of the branchial arches. The 3rd pharyngeal pouch was dissected at the 2nd and 4th clefts, and the neural tube and tissues surrounding the neural tube were removed **(**Figure 2.1A**)**. This left the third pharyngeal pouch, pharyngeal endoderm, surface ectoderm, and surrounding mesenchyme cells. At E11.25, because the third pharyngeal pouches make up a smaller proportion of the branchial arches and *Gcm2* expression is high, *Gcm2-eGFP* mice were used to identify and isolate the 3rd pharyngeal pouch and surrounding mesenchyme **(**Figure 2.1A**)**.

Cell disassociation and sc-RNAseq

Third pharyngeal pouches and surrounding tissues were dissected from E10.25 (33-36ss) and E11.25 (40-43ss) embryos. All tissues were dissected into PBS with 10%FBS on ice. Tissues were centrifuged, and PBS was replaced with a disassociation mix (0.7ug/mL Collagenase, 1.3ug/mL Hyaluronidase, 10%FBS in PBS). Cells were then disassociated at 37 degrees with frequent pipetting. Cells were filtered using a Flowmi Cell Strainer (40 micron). Cells were centrifuged and supernatant was replaced with 1mL of 0.05%BSA/PBS. Cells were centrifuged again and resuspended in 100uL 0.05%BSA/PBS. 10 uL of cells were mixed with an equal volume of Trypan blue and cell counts and viability were determined. Up to 1 mL of 0.05%BSA/PBS was added to cells and cells were centrifuged and resuspended in 0.05%BSA/PBS at a concentration of 1000 cells/uL. Cells were kept on ice between steps, and all centrifuge steps were done in a swinging bucket centrifuge at 4 degrees. Cells were then run through 10x Genomics Single Cell Gene Expression v3.1.

Single cell RNA-seq analysis

CellRanger count and CellRanger aggr were used to aggregate libraries, determine droplets that contain cells, and create a gene x cell matrix. Seurat was used to cluster cells and for all downstream analysis of scRNA-seq data (Butler et al., 2018; Hao et al., 2021; Satija et al., 2015; Stuart et al., 2019). Low quality cells and possible doublets were removed (number of UMIs <500 or >2000 and percent of mitochondrial reads < 10%). The effect of the cell cycle on clustering was regressed using Seurat's cell cycle regression method (Nestorowa et al., 2016). Cells were clustered and identified using marker genes. Differentially expressed transcription factors were identified using David Gene Ontology database to identify transcriptional regulators from differentially expressed genes. Differentially expressed signals from the mesenchyme were identified using David Gene Ontology terms "signal" and "differentiation." All codes used will be publicly available on Github.

Fluorescent in situ hybridization

Fluorescent *in situ* hybridizations were performed with ACD Bio RNAscope Fluorescent Multiplex V2. All probes used were standard probes from ACD Bio. Embryos were fixed for 16-28 hours in 4% PFA/PBS at room temperature. Embryos were dehydrated in an EtOH gradient, permeabilized in Xylene, and embedded in paraffin wax. Embryos were sectioned at 8 microns and proceeded to RNAscope Fluorescent Multiplex V2 pre-treatment protocol for FPPE samples(Wang et al., 2012). Antigen retrieval was performed for 15 minutes and Protease Plus was added for 30 minutes. All other steps were standard. All slides were imaged on a LSM 710 or LSM 880 confocal microscope.

Mice

All wild type mice were C57/BL6J from Jackson Laboratories. *R26iSmoM2* mice were kept homozygous and crossed to *Sox17-Cre* heterozygous mice for embryo experiments. Cre positive embryos were compared to Cre negative embryos. *Isl1*$^{fl/fl}$ mice were crossed to *Isl1*$^{fl/+}$*;Foxa2-Cre*$^{ER\ Cre/+}$ mice to create Cre positive and Cre negative *Isl1*$^{fl/fl}$ embryos. *Id4* knockouts were created using CRISPR/Cas9 with the following guide RNAs: TGTAGTCGATAACGTGCTGC and GAGCACGGCCACAGCCTGGG targeting the first exon. *Id4* mutants had a large deletion and frameshift (302 bps). Primers used to genotype embryos are listed in Table 2.1.

Results

Developmental timeline

Single cell RNA-seq was performed on embryos at E10.25 and E11.25, which spans the specification timeline of the thymus and parathyroids. At E10.25, the parathyroid is in the early stages of specification in the dorsal region of the 3rd pharyngeal pouch, as *Gcm2* expression is just starting to initiate. At this timepoint, the ventral region of the 3rd pharyngeal pouch expresses *Bmp4* and *Fgf8*, but has yet to express other thymus specific markers, notably, *Foxn1* (Chojnowski et al., 2014). At E11.25, the parathyroid is farther along the specification timeline, with *Gcm2* having been expressed for about a day, while thymus cells are likely more recently specified, as *Foxn1* has only been initiated in the ventral region for a few hours. At E11.25, the central region of the 3rd pharyngeal pouch does not express either *Foxn1* or *Gcm2*, and therefore has an unknown status of cell fate specification (Bain et al., 2016).

Cells from each timepoint cluster separately

Umaps of scRNA-seq at both timepoints show that there is little overlap between timepoints **(**Figure 2.1B**)**. We are confident in this result as it is likely that the transcriptomes of the 3rd pharyngeal pouch and surrounding mesenchyme change substantially over a day (as is confirmed by marker expression) and biological replicates from each timepoint cluster together. Along with the tissues of interest (3rd pharyngeal pouch, surface ectoderm, pharyngeal endoderm, and surrounding NCC mesenchyme), other tissues were identified, such as blood cells, neural tissue, and other tissues not near the third pharyngeal pouch and unlikely to contribute to 3rd pharyngeal pouch cell fate specification. To address the questions of interest of this study, cells belonging to the third pharyngeal pouch and its surrounding tissues were subsetted.

Identifying cell types

To identify candidate transcription factors driving thymus and parathyroid cell fate specification, as well as the heterogeneity of the developing 3rd pharyngeal pouch, clusters that are *Epcam* positive and *Neurod1* negative were subsetted and re-clustered **(**Figure 2.2A**)**. Within this population were some other cell types, such as thyroid (*Pax8* positive), 4th pharyngeal pouch cells (*Hoxc4* positive), and neural crest cells that may be early in the EMT process (marked by several mesenchyme markers). Third pharyngeal pouch cells were identified using several markers, including *Pax1, Pax9, Krt8,* and *Krt18.* At E10.25, the surface ectoderm contacts the ventral region of the 3rd pharyngeal pouch, and can be identified in this dataset through *Tfap2* and *Wnt6* expression. The dorsal side of the third pharyngeal pouch is attached to the pharynx at E10.25, and is just

starting to detach from the pharyngeal endoderm at E11.25. This cluster is identified by *Shh* and *Sox2* expression.

Heterogeneity of third pharyngeal pouch cells at E10.25 and E11.25

When cells from both timepoints are clustered together, there is little overlap between timepoints, consistent with the hypothesis that the 3rd pharyngeal pouch undergoes large transcriptional and cell fate specification changes between E10.25 and E11.25 **(**Figure 2.2A**)**. Because of the large differences, cells were re-clustered at each timepoint to address the heterogeneity at these timepoints. Re-clustering at each timepoint revealed more heterogeneity than seen when both timepoints were clustered together **(**Figure 2.2B,E**)**.

At E10.25, thyroid, 4th pharyngeal pouch, and NCCs were removed and the remaining cells were re-clustered, showing a surface ectoderm cluster, a pharyngeal endoderm cluster, and two 3rd pharyngeal pouch clusters **(**Figure 2.2B**)**. This is in contrast to the single E10.25 3rd pharyngeal pouch cluster identified when E10.25 and E11.25 cells were clustered together (Figure 2.2A). The ventral region of the third pharyngeal pouch was identified by the expression of *Fgf8*, while the dorsal region was identified by the expression of *Sox2* (Chojnowski et al., 2014; Wei & Condie, 2011). Interestingly, fluorescent *in situ* hybridization of two markers from the dorsal cluster of the third pharyngeal pouch show more heterogeneity than demonstrated in the scRNA-seq data at E10.5. While florescent *in situ* hybridization shows that *Sox2* is expressed in the dorsal, posterior region of the third pharyngeal pouch as previously described, the transcription factor, *Vgll2*, is expressed in the dorsal, anterior region (Figure 2.2D).

At E11.25, cells cluster into a small pharyngeal endoderm cluster, a parathyroid cluster (*Gcm2* and *Pth* positive), a thymus cluster (*Foxn1* positive), and a central cluster that is largely negative for *Gcm2* and *Foxn1* **(**Figure 2.2E**)**. The central cluster was not identified when E10.25 and E11.25 cells were clustered together **(**Figure 2.2A). A heatmap of top differentially expressed genes for each cluster show that while the thymus and parathyroid domains have distinct transcriptomes, the central cluster seems to share some attributes of both clusters (Figure 2.2F). Additionally, a small portion of cells in the central cluster express either *Foxn1* or *Gcm2,* and four central cells express both *Foxn1* and *Gcm2*, a phenomenon previously described at the protein level in cells at the border of the thymus and parathyroid domains (Bain et al., 2016) (Figure 2.2G). The central cluster is the largest cluster of cells in *Epcam* positive clusters at E11.25. However, fluorescent *in situ* hybridization for *Gcm2* and *Foxn1* at the same stage shows a small proportion of cells negative for both genes (Figure 2.2E). It is possible that this perceived infrequency of central cells expressing *Foxn1* or *Gcm2* in scRNA-seq is due an artifact of drop-out events. While the scRNA-seq data shows some genes expressed at a higher level in the central cluster, there are no markers that are exclusive to the central region, and such cells do not cluster with E10.25 cells, suggesting that these cells are likely specified into thymus or parathyroid cells, but have yet to express the full transcriptomes of either cell type.

Candidate cell autonomous specifiers of thymus and parathyroid cell fates

Identifying differentially expressed transcription factors

In order to identify candidate cell autonomous specifiers of the thymus and parathyroids, transcription factors were identified using gene ontology terms of

upregulated genes between the dorsal and ventral domains of E10.25 third pharyngeal pouch clusters and the thymus and parathyroid E11.25 clusters **(**Figure 2.3A**)**. While the list of differentially expressed genes look large when viewed on heatmaps as relative expression between clusters, most genes can be ruled out as candidate specifiers of the thymus or parathyroid based on their absolute expression. A specifier of the thymus or parathyroid cell fate would likely be exclusively expressed in one cell type or the other. However, most differentially expressed transcription factors are expressed at low levels, or high levels throughout cell types, but relatively higher in one or the other. Such transcription factors were not prioritized as candidate cell fate specifiers (Figure 2.11).

While the lists of differentially expressed transcription factors identified at E10.25 and E11.25 are large, only one transcription factor was identified as being differentially expressed at both timepoints, *Pax1* **(**Figure 2.3A**)**. This lack of overlap between timepoints further supports the hypothesis that cells at E11.25 are much further along the specification process and represent transcriptomes that are largely downstream of *Gcm2* and *Foxn1*. Therefore, differentially expressed transcription factors identified at E11.25 are likely not cell fate specifiers, and instead may be important in downstream function of the thymus or parathyroid. However, the function of two transcription factors that are differentially expressed at E11.25 were tested in thymus and parathyroid cell fate specification, *Isl1* and *Id4*. We generated standard and conditional mutant embryos for Id4 and Isl and analyzed patterning in the 3rdPP. We did not detect a patterning phenotype in these mutants indicating neither gene is involved in thymus or parathyroid specification (Figure 2.9).

Vgll2 and Sox2 serve as candidates of cell fate specification in the third pharyngeal pouch

Of the list of differentially expressed transcription factors identified at E10.25, only two showed high expression in the dorsal region of the pouch and low or absent expression in the ventral region: *Sox2* and *Vgll2* (Figure 2.3B,C). The role of *Sox2* as an inhibitor of differentiation has been well described in stem cells and makes it an interesting candidate in the 3rd pharyngeal pouch (Boyer et al., 2005; Takahashi & Yamanaka, 2006)**.** Fluorescent *in situ* hybridization of *Sox2* shows a dynamic expression pattern in the third pharyngeal pouch (Figure 2.3C). At E9.5, it is expressed throughout the endoderm and the third pharyngeal pouch. This is in contrast to a previously published paper which failed to detect *Sox2* expression in the third pharyngeal pouch at E9.5 using traditional *in situ* hybridization on whole mount embryos (Wei & Condie, 2011). At E10.5, *Sox2* is expressed in the dorsal region of the third pharyngeal pouch, but is restricted to the posterior region which is *Gcm2* negative at this timepoint. At E11.5, *Sox2* is restricted to the pharyngeal endoderm and is absent in the third pharyngeal pouch. These data suggest that *Sox2* may be an inhibitor of thymus and parathyroid cell fates. If true, this would also suggest that at E10.5, the ventral region of the third pharyngeal pouch is already specified, despite the absence of *Foxn1* expression.

The other candidate specifier of third pharyngeal pouch cell fates identified from the differentially expressed transcription factors at E10.25 is *Vgll2* (Figure 2.3B). The transcription factor, *Vgll2*, has been in its role as a differentiator of fast versus slow twitch muscle fibers (Hitachi et al., 2019; Honda et al., 2017). While whole mount *in situ* hybridizations have focused on its expression in somites, they also show dynamic

expression of *Vgll2* in the pharyngeal pouches. Using fluorescent *in situ* hybridization of *Vgll2* on sections, a more detailed expression pattern was observed. At E9.5, *Vgll2* is expressed in the anterior region of the third pharyngeal pouch, in the presumptive parathyroid domain. At E10.5, *Vgll2* is expressed in the dorsal, anterior region of the third pharyngeal pouch, overlapping *Gcm2* expression, but also extends to some *Gcm2* negative cells. At E11.5, *Vgll2* expression is not detected in the third pharyngeal pouch. The transient expression of *Vgll2*, initiating prior to *Gcm2* expression and being downregulated following *Gcm2* expression, makes it a strong candidate as a specifier of the parathyroid cell fate.

Vgll2 and Sox2 have different expression patterns in constitutively active Smo model

In order to support or rule out *Sox2* and *Vgll2* as candidate specifiers of 3rd pharyngeal pouch cell fates, we observed their expression in a mouse model with known changes to *Gcm2* and *Foxn1* expression. In mice with ectopic expression of a constitutively active Smoothened allele (*R26iSmom2;Sox17-Cre*), *Foxn1* expression is restricted to the ventral region of the third pharyngeal pouch, *Gcm2* expression remains unchanged, while cells in the central zone remain negative for *Gcm2* and *Foxn1*. The restriction of *Foxn1* expression in the SmoM2 model has been hypothesized to be due to the expansion of *Tbx1*, which inhibits *Foxn1* expression. However, previous studies have not been able to explain why *Gcm2* expression does not expand into the central, *Tbx1* positive region of the third pharyngeal pouch (Bain et al., 2016).

In E11.5 *R26iSmom2;Sox17-Cre* embryos, *Vgll2* was not observed in the central region of the third pharyngeal pouch (Figure 2.4A). This suggests that either *Vgll2* is not driven by SHH, or that it is inhibited by another factor. However, this result supports

Vgll2 as a candidate parathyroid cell fate specifier. If it were the specifier and was expressed in the central region of the third pharyngeal pouch one would also expect *Gcm2* to be expressed in this region. On the other hand, *Sox2* expression was observed in the *Gcm2/Foxn1* negative regions of the third pharyngeal pouch of E11.5 *R26iSmom2;Sox17-Cre* embryos (Figure 2.4B). Based on this result, we hypothesized that either the central region of the third pharyngeal pouch in *R26iSmom2;Sox17-Cre* embryos is converted into a more pharynx like state, or that they retain the third pharyngeal pouch identity but fail to express *Gcm2* or *Foxn1* in the central cells due to prolonged *Sox2* expression. To delineate between these two hypotheses, we observed the pharyngeal pouch specific marker, *Pax1* in E11.5 *R26iSmom2;Sox17-Cre* embryos. *Pax1* expression was observed throughout the third pharyngeal pouch in *R26iSmom2;Sox17-Cre* embryos, including the *Gcm2/Foxn1* negative cells, suggesting that these cells retain their third pharyngeal pouch identity, but fail to specify into thymus or parathyroid (Figure 2.4C). Taken together, these results support *Vgll2* as a candidate parathyroid cell fate specifier and suggest that *Sox2* inhibits cell fate specification in the third pharyngeal pouch.

Heterogeneity of NCC mesenchyme at E10.25 and E11.25

The diversity of NCC mesenchyme increases dramatically between E10.25 and E11.25. At E10.25, there are only three mesenchyme populations nearby the third pharyngeal pouch (Figure 2.5B). E10.25 mesenchyme clusters 4, 5, and 6 are far away from the third pharyngeal pouch, and likely represent NCCs earlier in migration. E10.25 mesenchyme 1, 2, and 3 are located around the third pharyngeal pouch. However, E10.25 mesenchyme 2 and 3 clusters are distinguished by differential expression of histones, and

likely do not represent distinct biological cell types. It is possible that the differential expression of histones is due to cells being in different phases of the cell cycle, despite the cell cycle being regressed during clustering. Using *Gata6* as a marker of E10.25 mesenchyme 1 and *Barx1* as a marker of E10.25 mesenchyme 2/3, we used FISH to identify the spatial locations of each cluster. While *Barx1* is located surrounding the third pharyngeal pouch, *Gata6* expression is slightly removed from the third pharyngeal pouch, suggesting E10.25 mesenchyme 2/3 surround the third pharyngeal pouch, separating the third pharyngeal pouch from E10.25 mesenchyme 1 (Figure 2.5B).

While the mesenchyme at E10.25 is low in diversity, the mesenchyme at E11.25 has more diversity than previously known. At E11.25, scRNA-seq data shows 6 clusters of mesenchyme. Again, using markers of each cluster, we mapped the clusters around the third pharyngeal pouch. While E11.25 Mesenchyme 5/6 were not located around the third pharyngeal pouch, E11.25 mesenchyme 1, 2, 3, and 4 formed distinct regions around the third pharyngeal pouch on the dorsal-ventral and anterior-posterior axis (Figure 2.5C). Viewing the E11.25 mesenchyme markers at E10.5 shows a dynamic expression pattern of such markers. While *Dlx5*, *Hand2/Gata6,* and *Six1* show distinct expression domains around the third pharyngeal pouch at E11.5, *Dlx5* and *Hand2* are expressed ubiquitously in the mesenchyme at E10.5, while *Six1* and *Gata6* are not expressed directly next to the third pharyngeal pouch (Figure 2.5D). These dynamic expression patterns and increase in mesenchyme diversity suggest that the mesenchyme diversifies after third pharyngeal pouch cell fate specification.

Candidate signals driving thymus and parathyroid cell fates

Differentially expressed signals from the neural crest mesenchyme

Signals driving the thymus and parathyroid are likely to come from the surrounding neural crest mesenchyme, pharyngeal endoderm, and the surface ectoderm, and would likely be expressed exclusively adjacent to either the thymus or parathyroid domains. To identify candidate signals driving each cell fate, we used gene ontology terms to identify which differentially expressed genes are associated with signaling and differentiation. The lists of differentially expressed signals from the mesenchyme was large, but the most striking differentially expressed signal was *Tgfb2* (Figure 2.10). Fluorescent *in situ* hybridizations of *Tgfb2* showed that it is expressed around the thymus domain at E11.5, but widely expressed at E10.5 (Figure 2.6A). This result along with the lack of diversity of the mesenchyme at E10.25 and the fact that mice that lack NCC mesenchyme around the third pharyngeal pouch in *Splotch* mutants express both *Foxn1* and *Gcm2* suggest that the key signals driving initial thymus and parathyroid cell fate specification are not located in the NCC mesenchyme (Griffith et al., 2009).

Differentially expressed signals from pharyngeal endoderm and surface ectoderm

To identify signals from tissues other than the NCC mesenchyme, we focused on differentially expressed signals at E10.25 in the pharyngeal endoderm, which contacts the presumptive parathyroid domain, and the surface ectoderm, which contacts the presumptive thymus domain prior to *Foxn1* expression. The list of differentially expressed signals from the pharyngeal endoderm and surface ectoderm is much smaller than the mesenchyme lists (Figure 2.6B). Several signals in our candidate gene list have

been previously identified and tested, including *Bmp4*, *Fgf8*, and *Shh*. Interestingly, *Shh* is the only signal specifically expressed in the pharyngeal endoderm (Figure 2.6B).

The surface ectoderm expresses *Wnt4* and *Wnt6*, which may signal to the 3rd PP (Figure 2.6C). Previous studies have shown that WNTs drive *Foxn1* expression in cultured thymic epithelial cells (Balciunaite et al., 2002). The temporal-spatial expression of *Wnt4* and *Wnt6*, along with the fact that WNTs can drive *Foxn1* expression after specification makes WNTs a candidate signal driving the thymus cell fate. Building on this hypothesis, the parathyroid may need to inhibit the WNT signal response to be specified into parathyroid cells. Our scRNA-seq dataset shows the expression of two negative modulators of WNT signal response in the 3rd PP: *Sfrp2* and *Shisa2* (Bafico et al., 1999; Furushima et al., 2007; Liang et al., 2019) (Figure 2.6B,C). While *Shisa2* is expressed throughout the 3rd PP and pharyngeal endoderm, *Sfrp2* is restricted to the dorsal region of the 3rd PP at E10.5, suggesting it may inhibit WNT signal response in the parathyroid domain. Consistent with this hypothesis, fluorescent *in situ* hybridization shows *Sfrp2* is expressed in the 3rd PP at E9.5, before parathyroid cell fate specification (Figure 2.6C). By E11.5, after thymus and parathyroid specification, *Wnt4* is expressed in the thymus domain, but *Sfrp2* is no longer expressed, suggesting inhibition of Wnt response may not be necessary for maintenance of the parathyroid cell fate. *Shisa2* is expressed throughout the 3rd PP at E10.5 and E11.5, suggesting it may not play a substantial role in modulating the WNT response (Figure 2.6B).

To test the role of *Sfrp2* and WNT signaling in the specification of the parathyroid and thymus cell fates, we observed *Gcm2* and *Foxn1* expression in mice with ectopic expression of *Sfrp2* throughout the pharyngeal endoderm and third pharyngeal pouch. At

E11.5, *R26Sfrp2* mice express both *Foxn1* and *Gcm2* (Figure 2.6D). This suggests that either *Sfrp2/Wnts* do not regulate third pharyngeal pouch cell fates, or that transgenic *Sfrp2* expression is not sufficient to inhibit *Foxn1* expression or a WNT response.

Discussion

Dynamic transcriptomes of the third pharyngeal pouch

This study sought to answer the longstanding questions of what signals and transcription factors are responsible for the specification of the thymus and the parathyroid. While several signals have been shown to play a role in 3rd PP cell fate specification, none have been shown to be the sole driver of either cell fate. Additionally, although several transcription factors have been shown to have differential expression prior to *Gcm2* or *Foxn1*, none of the transcription factors tested so far have caused a loss of the thymus or parathyroid individually, suggesting the specifier or either cell fate has yet to be identified. In this study, we tested two transcription factors that are differentially expressed at E11.5, *Id4* and *Isl1*. However, neither mutant had a phenotype in the 3rd PP at E11.5, suggesting neither are the specifiers of the thymus or parathyroid. Additionally, *Id4* and *Isl1* expression at E10.5 is ubiquitous throughout the 3rd PP, pharyngeal endoderm, and surface ectoderm. In fact, all genes that are differentially expressed at E11.5 are expressed throughout the 3rd PP at E10.5 or not expressed at all, suggesting the differential expression of transcription factors identified at E11.25 is largely due to the transcriptomes changing post-specification.

Because the transcriptomes identified at E11.25 likely represent cells that are already specified and in the process of differentiating into mature organs, differentially

expressed transcription factors at E11.25 are much more likely to be the specifiers of 3rd PP cell fates. Despite this, almost all differentially expressed transcription factors at E10.25 were either very lowly expressed or not specific to one 3rd PP domain over the other. This resulted in a very small final candidate gene list for 3rd PP cell fate specifiers consisting of only *Vgll2* and *Sox2*.

Vgll2 is a candidate specifier of the parathyroid cell fate

The transcription factor, *Vgll2*, has not been widely studied, with most research in mice focusing on its role in differentiating slow and fast twitch muscle fibers (Hitachi et al., 2019; Honda et al., 2017). However, its expression in the pharyngeal pouches has not been described. We show here that *Vgll2* is not only co-expressed with *Gcm2* at E10.25, but precedes its expression as early as E9.5. By E11.25, *Vgll2* is not detected in the 3rd PP, suggesting it may be necessary for parathyroid cell fate specification, but not the maintenance of the parathyroid cell fate. Additionally, *Vgll2* is expressed in some *Gcm2* negative cells at E10.25, suggesting that some cells are still being specified into the parathyroid at this timepoint, but have yet to express previously identified parathyroid markers. In any case, it does not appear that *Vgll2* is expressed in the presumptive thymus domain at any stage, supporting the hypothesis that it is a candidate parathyroid cell fate specifier. In other tissues, VGLL2 has been shown to interact with TEAD transcription factors, of which are expressed in the 3rd PP according to our scRNA-seq data (Data not shown). To further support *Vgll2* as a candidate parathyroid cell fate specifier, we observed its expression in R26SmoM2 embryos. If *Vgll2* is the specifier of the parathyroid and is upstream of *Gcm2*, we would not expect the Vgll2+ domain to expand

into the *Gcm2* negative regions of SmoM2 embyos. In fact, there was no ectopic *Vgll2* expression in R26SmoM2 embryos, supporting the hypothesis that it is a parathyroid cell fate specifier.

Sox2 is a candidate inhibitor of the thymus and parathyroid cell fates

The only other transcription factor that was differentially expressed at E10.25 between the two 3rd PP domains was *Sox2*, a Yamanaka factor that has been well studied in its role keeping stem cells pluripotent. If *Sox2* has a similar role in the 3rd PP, we would expect that it would inhibit thymus and parathyroid cell fate specification. Sox2 had a dynamic expression pattern in the third pharyngeal pouch, being expressed widely at E9.5 prior to known marker gene expression, and being restricted to the dorsal domain at E10.25, but not co-expressed with *Gcm2*. By E11.25, when cells are likely already specified, *Sox2* is not detected in the third pharyngeal pouch. While *Sox2* expression has been described in the 3rd PP in a previous publication, it was observed using colorimetric *in situ* hybridization on whole mount or embryo sections (Wei & Condie, 2011). Here, we show a different expression pattern using a more sensitive method that allows us to multiplex as well.

In R26SmoM2 embryos, *Sox2* expression is detected in the *Gcm2* and *Foxn1* negative cells. Because *Sox2* is also expressed in the pharyngeal endoderm, it is possible that driving an ectopic SHH activity in the third pharyngeal pouch results in some cells trans-differentiating into pharynx cells. However, because the pouch marker, *Pax1*, was detected throughout the 3rd PP in R26SmoM2 embryos, we are confident that the cells retain their 3rd PP identity. This would suggest that *Sox2* inhibits thymus and parathyroid

cell fate specification, and the ectopic expression of *Sox2* in response to forced SHH pathway activity is responsible for the failure of *Gcm2* to expand into the *Tbx1* positive, *Foxn1* negative cells.

Timing of thymus and PT cell fate specification may occur sooner than previously thought

The dynamic expression pattern of *Sox2* in the third pharyngeal pouch may also speak to the timing of thymus and parathyroid cell fate specification. At E9.5, the candidate parathyroid cell fate specifier, *Vgll2* is expressed in the presumptive parathyroid domain, but is also expressed with *Sox2*, which may explain why *Gcm2* is not detected at E9.5. By E10.5, *Sox2* is not detected in *Gcm2* positive cells, but is also not detected in the ventral, presumptive thymus domain of the 3rd PP. If *Sox2* is responsible for preventing thymus and parathyroid cell fate specification, this result would suggest that the thymus domain begins specifying as much as a full day before *Foxn1* expression is detected. Indeed, a previous study showing the expression of *Foxn1* in a pharynx removed at E9.5 and cultured under a kidney capsule suggests that the cells are competent to specify the thymus cell fate early (Gordon et al., 2004).

NCC mesenchyme undergoes large changes between E10.25 and E11.25 and expresses Tgfb2

To identify signals that may drive the thymus and parathyroid cell fates, we focused on three major signaling centers around the third pharyngeal pouch: the pharyngeal endoderm, surface ectoderm, and neural crest mesenchyme. Single cell RNA-

seq of the neural crest mesenchyme shows large changes to the heterogeneity over the timeline of specification. At E10.25, There appears to be one major cluster marked by *Barx1* surrounding the third pharyngeal pouch. Two other clusters marked by *Gata6* are present farther away from the 3rd PP. However, these two clusters are mostly distinguished on scRNA-seq by differential expression of histone genes, and likely do not represent two biologically different cell types. It is possible that each cluster represents the same cell type in different phases of the cell cycle. Although the cell cycle was regressed from clustering using Seurat's cell cycle regression pipeline, it does not remove or regress differential expression of histone genes specifically (Nestorowa et al., 2016). At E11.25, the NCC mesenchyme increases in diversity, with four cell types spatially located around the 3rd PP. Marker genes of different E11.25 mesenchyme clusters are either widely expressed at E10.25, or absent. Specifically, *Hand2* and *Dlx5* are widely expressed at E10.25. In other pharyngeal arches, these two genes have been shown to regulate each other in the mesenchyme, which may partially explain the increase in diversity seen at E11.25 (Barron et al., 2011; Vincentz et al., 2016). We cannot, however, rule out the possibility that signals from the 3rd PP itself contribute to such diversification of the mesenchyme.

Identifying differentially expressed signals from the neural crest mesenchyme that may drive 3rd PP cell fates proved difficult as the list was very large. However, one signal that stood out was *Tgfb2*, which is widely expressed at E10.25, but becomes restricted around the thymus domain by E11.5. While it is not known whether the 3rd PP responds to TGFB2, it may be involved in driving third PP cell fates. However, because previous studies have shown that the NCC mesenchyme provides a signal driving cell fates in the

central region of the 3rd PP but is not necessary for the initiation of the thymus and PT cell fates, we decided to focus more on differentially expressed signals from the pharyngeal endoderm and surface ectoderm (Griffith et al., 2009).

WNTs and a WNT inhibitor are candidate signals driving thymus and PT cell fates

At E10.25, the 3rd PP is contacted by two tissues that could serve as the major signaling centers driving thymus and PT cell fates. The dorsal domain is contacted by the pharyngeal endoderm, which has been shown to provide SHH as an inductive signal driving the parathyroid cell fate (Moore-Scott & Manley, 2005). At this time point, the ventral domain is contacted by the surface ectoderm. While no studies have shown an importance of the surface ectoderm for driving the thymus cell fate, its proximity to the presumptive thymus domain and the unimportance of NCC mesenchyme for driving initial thymus cell fates suggests it may provide signals driving the thymus cell fate. The timing of the surface ectoderm contacting the ventral thymus domain also loosely coincides with the timing of *Sox2* downregulation in the ventral 3rd PP. *Bmp4* is expressed in the surface ectoderm, but its role in thymus cell fate specification remains unknown as previous studies disrupted *Bmp4* in the ventral 3rd PP and NCC mesenchyme, but such studies did not disrupt *Bmp4* in the surface ectoderm as well (Gordon et al., 2010; Patel et al., 2006). This may explain why such mice maintained *Foxn1* expression

We identified an additional signal from the surface ectoderm at E10.25, *Wnt4* and *Wnt6*. A previous study has shown that WNTs are capable of driving *Foxn1* expression. However, this study was done on cultured thymic epithelial cells from a differentiated thymus, and do not address the role of WNTs in the initial specification of the thymus

cell fate. The proximity of WNTs to the thymus as *Sox2* is being downregulated, and prior to *Foxn1* initiation makes them good candidates driving the thymus cell fate.

In the dorsal region of the pouch, the WNT response inhibitor, *Sfrp2*, is expressed. While *Sfrp2* expression does not overlap with *Gcm2* expression at E10.5, studies in other tissues have demonstrated that it can work non-cell autonomously to inhibit a WNT response (Ladher et al., 2000; Liang et al., 2019; Mirotsou et al., 2007). Additionally, *Sfrp2* is expressed throughout the third pharyngeal pouch at E9.5. This dynamic expression pattern suggests that it may inhibit a WNT response early. By E10.5, when *Gcm2* is expressed, it may not be necessary for maintenance of the parathyroid cell fate, and thus not expressed in the parathyroid. Similarly, if the thymus domain responds to WNTs at E10.5, one would not expect *Sfrp2* to be expressed in the ventral thymus domain.

The lack of *Sfrp2* expansion into the *Gcm2* negative, *Foxn1* negative regions in R26SmoM2 embryos may partially explain why *Gcm2* does not expand into this region, as these cells are forced to respond to SHH, but may see conflicting WNT signals without a WNT inhibitor. Nevertheless, overexpression of *Sfrp2* throughout the 3rd PP did not cause a loss of *Foxn1* that may be expected if cells are unable to respond to WNTs. This may be due to two reasons. First, that our hypothesis is wrong, and WNT signaling is not necessary for driving the thymus cell fate. Second, *Sfrp2*, while having a role in inhibiting WNT signaling in other tissues, may not have the same role in the 3rd PP, or may not be sufficient to inhibit the WNT response alone. Future experiments to address the role of WNT signaling in the 3rd PP may benefit from a more robust knockdown of the WNT response.

Lack of thymus specifier

One goal of this project that was not met was identifying a candidate thymus specifier. While *Isl1* was a candidate from the E11.25 dataset, it had widespread expression at earlier timepoints, making it a weaker candidate, and *Isl1* cKO's did not lose *Foxn1* expression. ScRNA-seq data from E10.25 did not identify a transcription factor specific to the presumptive thymus domain, and all transcription factors identified as specific to the thymus domain at E11.25 are ubiquitously expressed in the 3rd PP at E10.5 or not expressed at all, ruling many of them out as good candidate thymus specifiers.

One reason we may not have identified a candidate thymus cell fate specifier is that it could be very transiently expressed (Figure 2.8). Several other transcription factors have presented dynamic, transient expression (see *Sox2* and *Vgll2* expression). It is possible that the thymus specifier is expressed between E10.25 and E11.25, but not during those timepoints that were captured in scRNA-seq. The lack of *Sox2* expression in the ventral domain at E10.5 suggest that the thymus domain may have begun specification, but the actual transcription factor upstream of *Foxn1* may not be expressed until late E10.75-E11. Once Foxn1 is expressed and the thymus is specified, the specifier of the thymus may not be necessary for maintenance of the thymus cell fate, and may be downregulated by E11.25, the second timepoint of our scRNA-seq experiments.

Another possibility of why we were unable to identify a candidate thymus specifier is that the thymus specifier may be expressed throughout the third pharyngeal pouch, but only active in the presumptive thymus domain. In this case, we would not identify it as we focused on transcription factors that are differentially expressed between

3rd PP clusters. A downside to transcriptomic experiments is the lack of knowledge of the state of proteins in cells. The thymus specifier may undergo post-transcriptional modifications and is only active in one cell type despite being ubiquitously expressed. Both WNT signaling and BMP signaling act through activation of proteins that are present in cells responding to signals and those not responding. Downstream targets of WNT and BMP signaling vary between tissues, making it hard to identify cells in our datasets that are responding to such signals. However, it is possible that the thymus cell fate is specified directly through SMADs activated by BMP signaling or B-catenin/TCF4/Lef1 activated by WNT signaling.

Overall, this study identified several new candidate genes that may play a role in thymus and parathyroid cell fate specification (Figure 2.7). First, we identified *Sox2* as a candidate negative regulator of thymus and parathyroid cell fates. Second, we identified *Vgll2* as a candidate specifier of the thymus cell fate. And third, we identified WNT signaling and the WNT inhibitor, *Sfrp2* as a candidate signaling pathway driving 3rd PP cell fates. Future studies following up on these candidate genes could further increase our knowledge of how the thymus and parathyroids are specified.

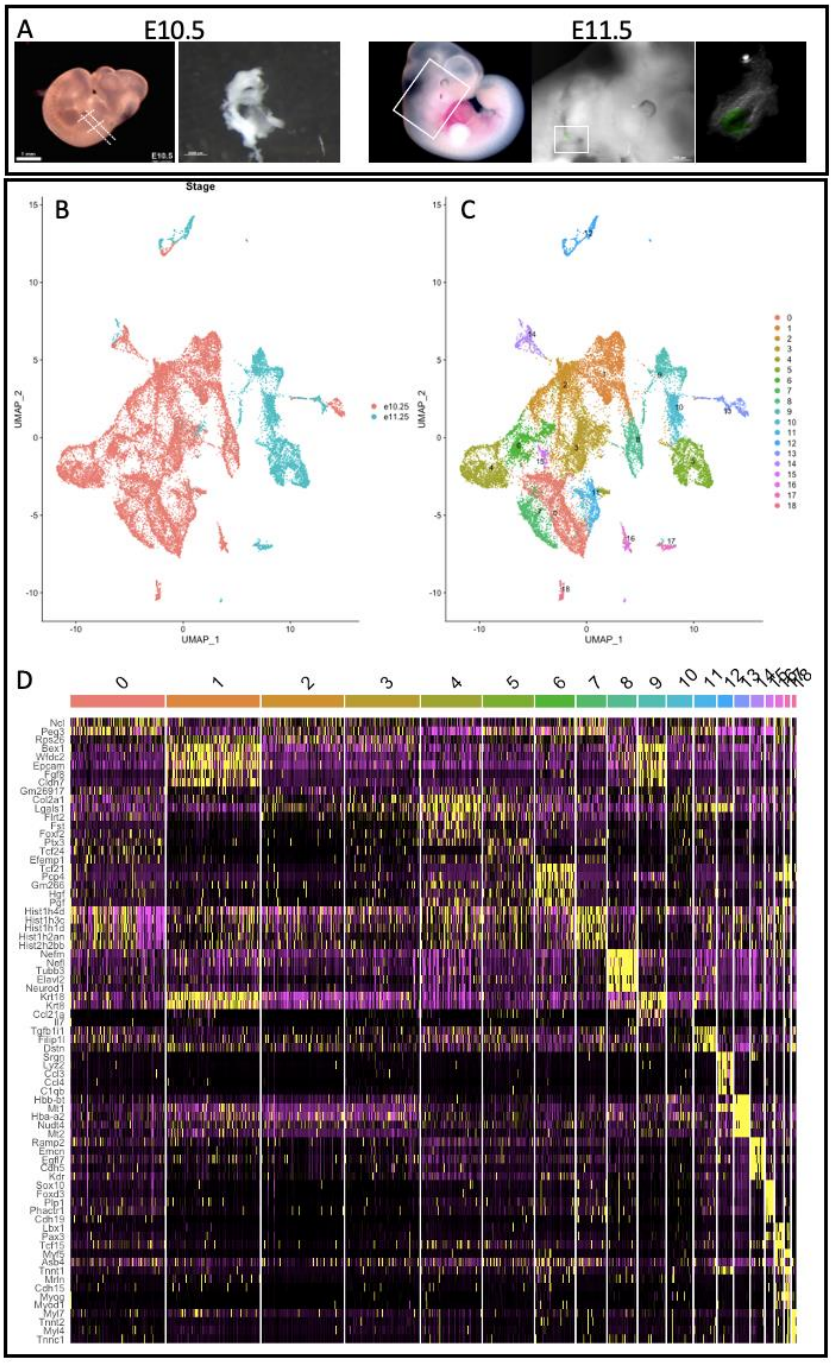

Figure 2.1. Overview of scRNA-seq on 3rd PP and surrounding cells at E10.25 and E11.25. A) Dissections of 3rd PP and surrounding cells. B) Clustering of all cells from E10.25 and E11.25 do not cluster together. C) Clusters of all cells from E10.25 and E11.25. D) Top marker genes of each cluster.

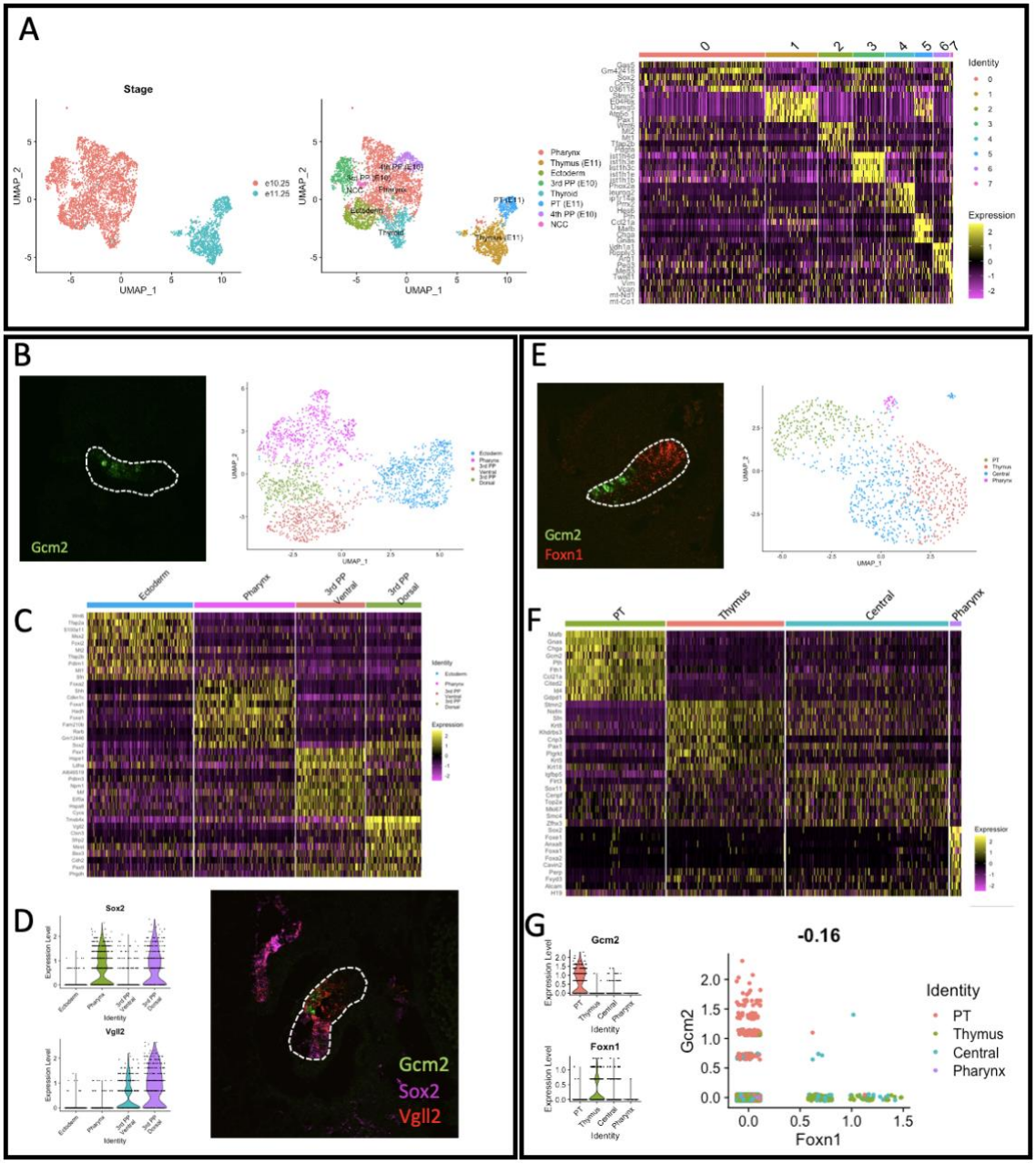

Figure 2.2. Re-clustered *Epcam* positive cells. A) Umaps of cells from E10.25 and E11.25 and heatmap of top markers for each cell type show that cells cluster separately based on timepoints. B,E) Umaps of re-clustered *Epcam* positive cells from E10.25 (B) and E11.25 (E), with florescent *in situ* hybridization of representative sections at each timepoint. C,F) Top marker genes of each cluster at E10.25 (C) and E11.25 (F). D) Expression of *Gcm2*, *Sox2*, and *Vgll2* at E10.25 shows more diversity than observed in

scRNA-seq. G) Some central cluster cells express either *Gcm2* or *Foxn1*, with only 5 cells expressing both genes.

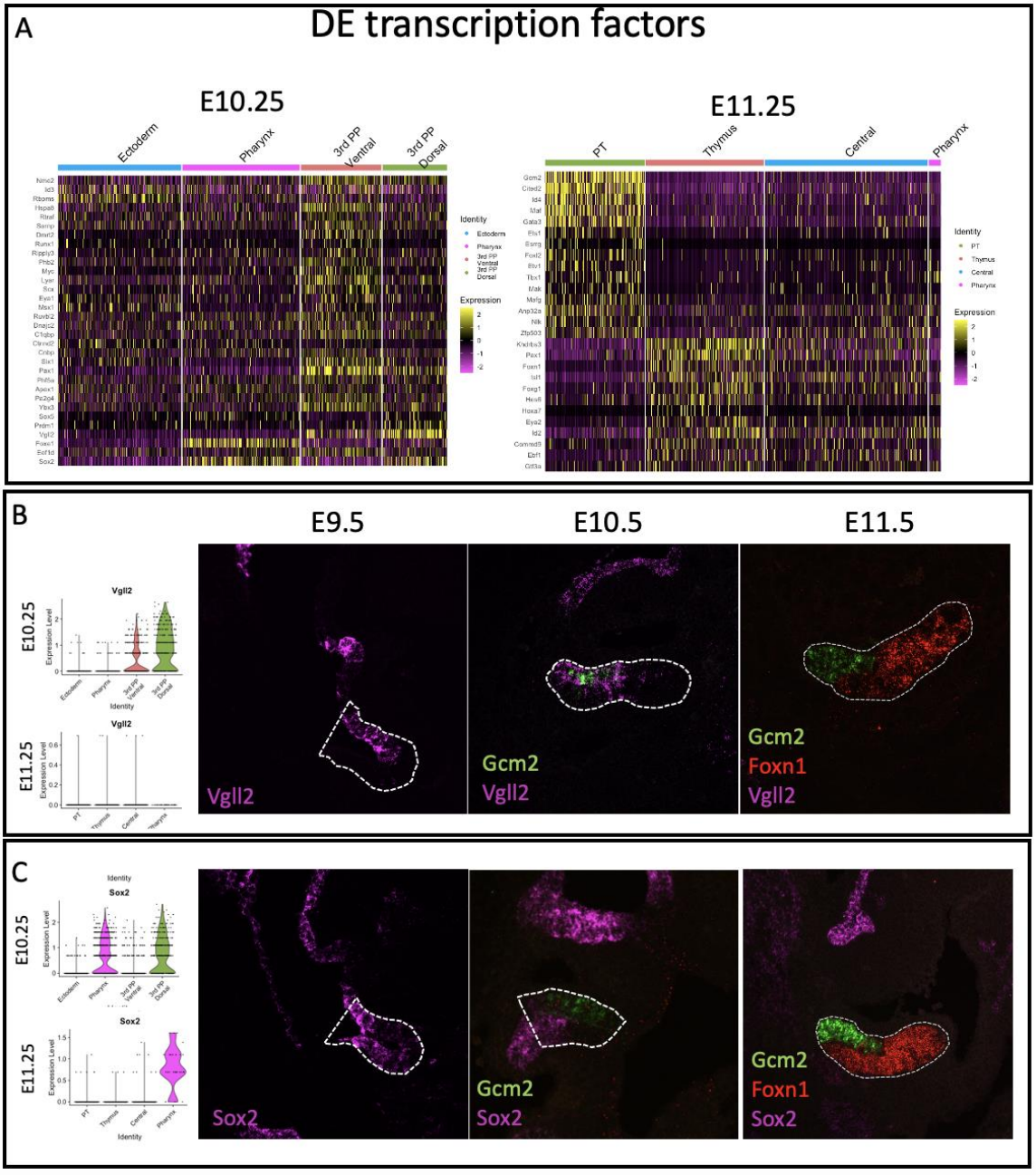

Figure 2.3. *Vgll2* and *Sox2* are candidate transcription factors regulating thymus and parathyroid cell fates. A) Differentially expressed transcription factors at E10.25 and E11.25. B) Expression of *Vgll2* between E9.5 and E11.5. *Vgll2* expression precedes *Gcm2* expression but is downregulated by E11.25. C) Expression of *Sox2* from E9.5-

E11.5. *Sox2* is widely expressed in the 3rd PP at E9.5, downregulated in the ventral domain and *Gcm2* positive cells by E10.5, and is only expressed in the pharynx by E11.5.

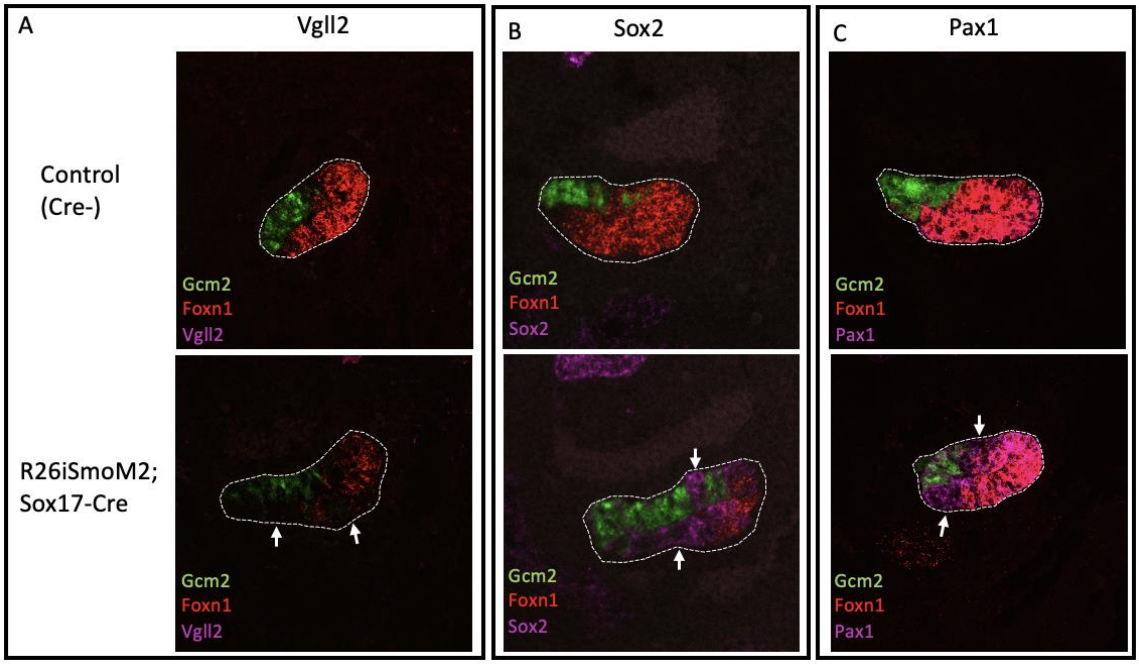

Figure 2.4 Fluorescent *in situ* hybridization of *Vgll2*, *Sox2*, and *Pax1* in E11.5 SmoM2 embryos. A) *Vgll2* expression is not expanded in response to ectopic SHH signaling. B) Ectopic *Sox2* expression in *Gcm2/Foxn1* negative cells in *R26iSmoM2* embryos. C) The universal pharyngeal pouch marker, *Pax1*, is not downregulated in *R26iSmoM2* embryos.

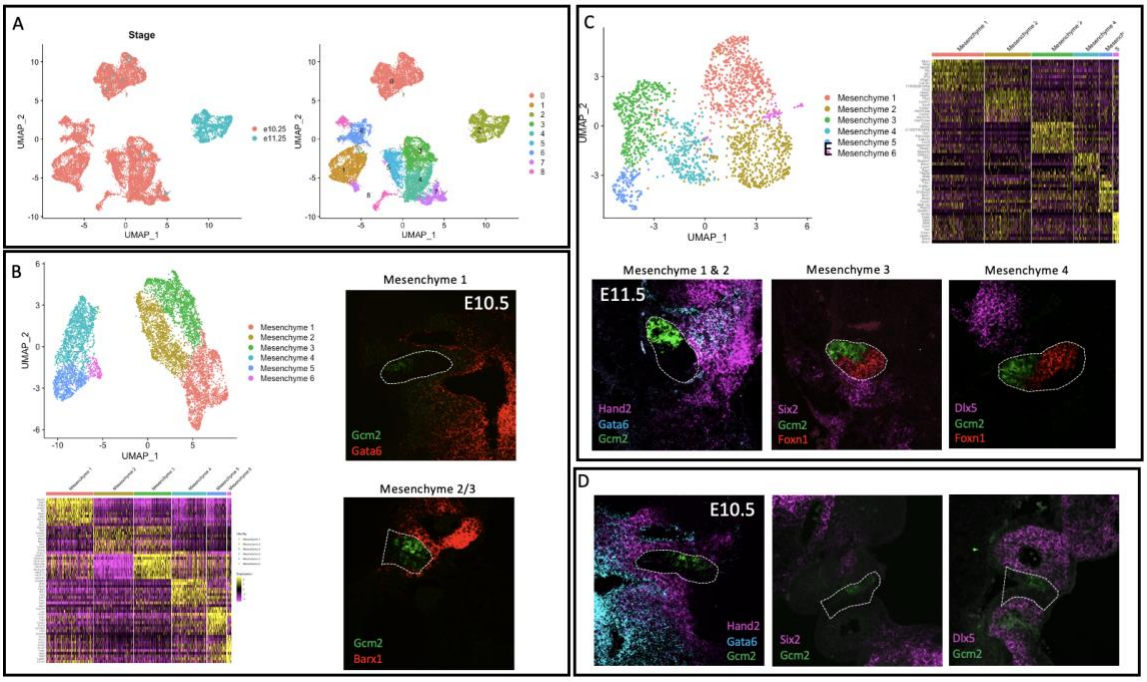

Figure 2.5. NCC mesenchyme diversity surrounding the 3rd PP. A) NCC mesenchyme clusters separately based on developmental stage. B) E10.25 NCC mesenchyme forms six clusters. Mesenchyme 4/5/6 express markers expressed closer to the neural tube (data not shown). Mesenchyme 2/3 are only separated by differential expression of Histone genes. Mesenchyme 1 (*Gata6*) is not directly adjacent to the 3rd PP. Mesenchyme 2/3 (*Barx1*) is located around the 3rd PP at E10.25. C) E11.25 mesenchyme forms six clusters. Mesenchyme 5/6 are not located nearby the 3rd PP (data not shown). E11.25 Mesenchyme 1 (*Hand2/Gata6*) and Mesenchyme 2 (*Hand2*) are expressed central/anterior and ventral/anterior to the 3rd PP. Mesenchyme 3 (*Six2*) is located ventral/posterior of the 3rd PP. Mesenchyme 4 (*Dlx5*) is dorsal/anterior of the 3rd PP. D) E11.25 mesenchyme markers are widely expressed (*Hand2* and *Dlx5*) or not expressed (*Six2*) around the 3rd PP at E10.5.

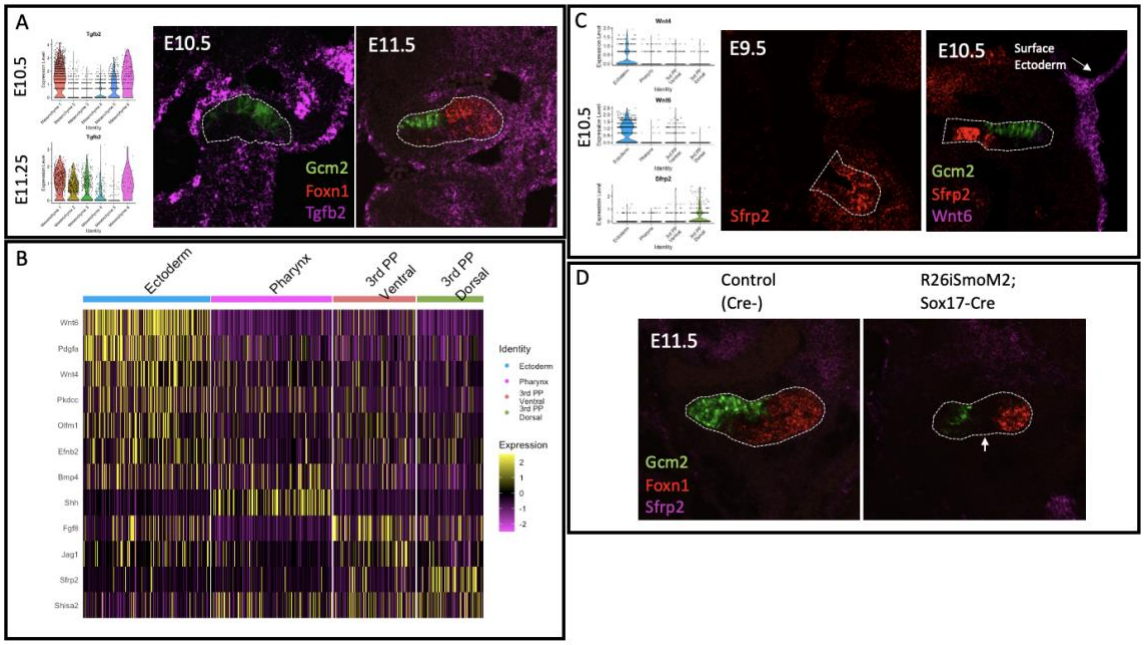

Figure 2.6. Candidate Signals driving thymus and PT cell fates. A) *Tgfb2* is expressed around the thymus domain at E11.5, but is widely expressed in the NCC mesenchyme at E10.25. B) Differentially expressed signals in *Epcam* positive cells at E10.25. C) Fluorescent *in situ* hybridization confirms the expression of *Wnt6* in the surface ectoderm and the WNT inhibitor, *Sfrp2*, in the dorsal/posterior region of the 3rd PP at E10.5. *Sfrp2* is widely expressed at E9.5. D) SHH does not drive *Sfpr2* at E11.5 in *R26iSmoM2* embryos.

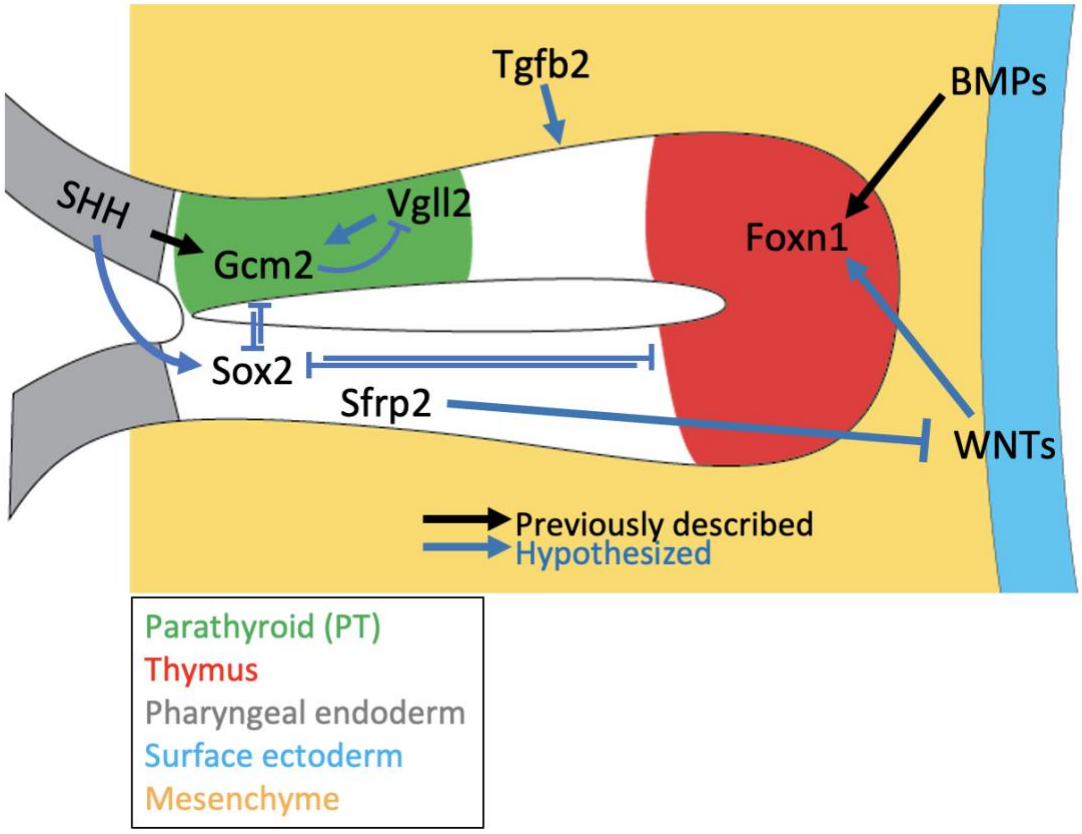

Figure 2.7 New model of 3rd PP cell fate specification. SHH drives *Gcm2*, while BMPS drive *Foxn1*. Added to the model are *Vgll2* as a candidate parathyroid cell fate specifier and *Sox2* as an inhibitor of thymus and parathyroid cell fates. *Wnt4/6* are added as a candidate driver of the thymus cell fate, with *Sfrp2* inhibiting the WNT signal in the dorsal region.

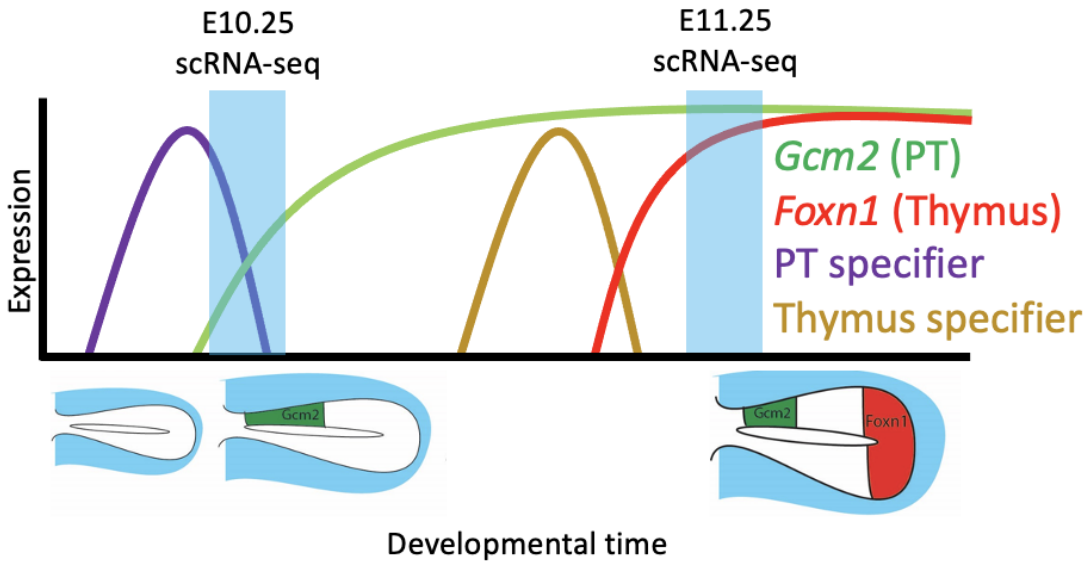

Figure 2.8. Possible transient expression of thymus and parathyroid cell fate specifiers. The candidate parathyroid specifier (*Vgll2*) is transiently expressed before and slightly after *Gcm2* is expressed and was identified in our E10.25 scRNA-seq timepoint. If the thymus cell fate specifier is also transiently expressed prior to *Foxn1* initiation, it may have only been expressed between E10.25 and E11.25 scRNA-seq experiments.

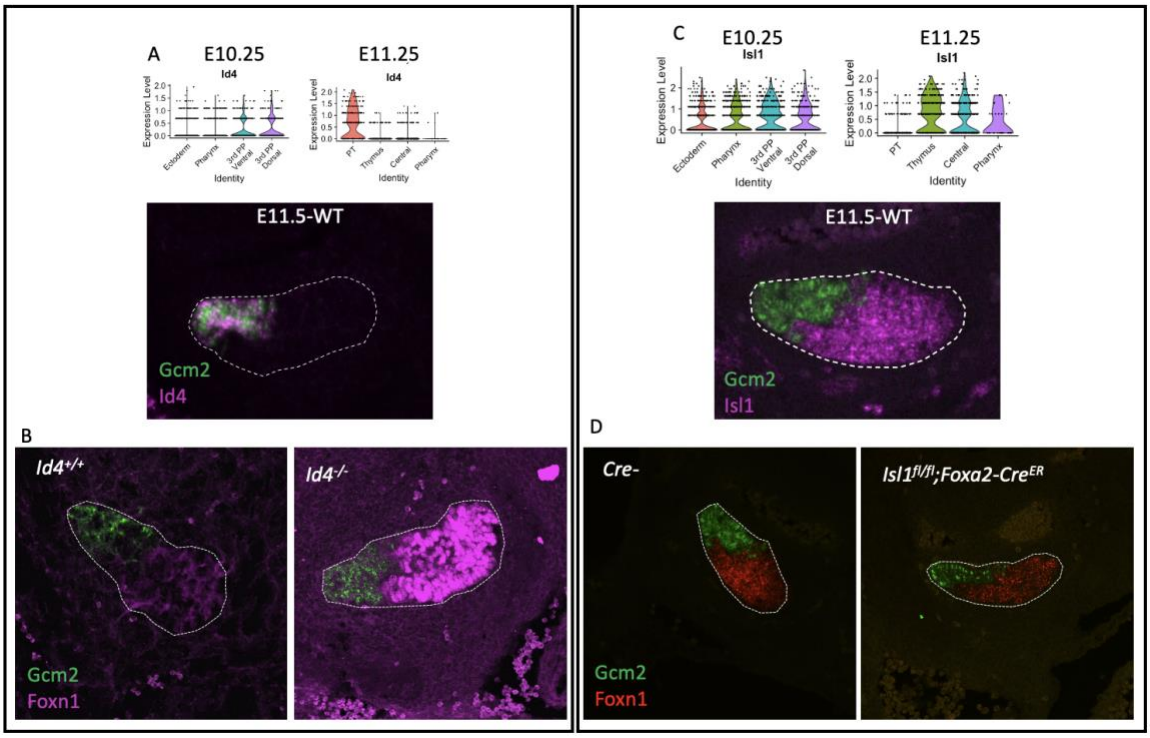

Figure 2.9. *Isl1* and *Id4* are not candidate thymus or parathyroid cell fate specifiers.

A,C) *Id4* and *Isl1* are expressed in the parathyroid at E11.5, but are widely expressed at E10.25. B,D) *Id4* and *Isl1* mutant embryos express *Foxn1* and *Gcm2* at E11.5

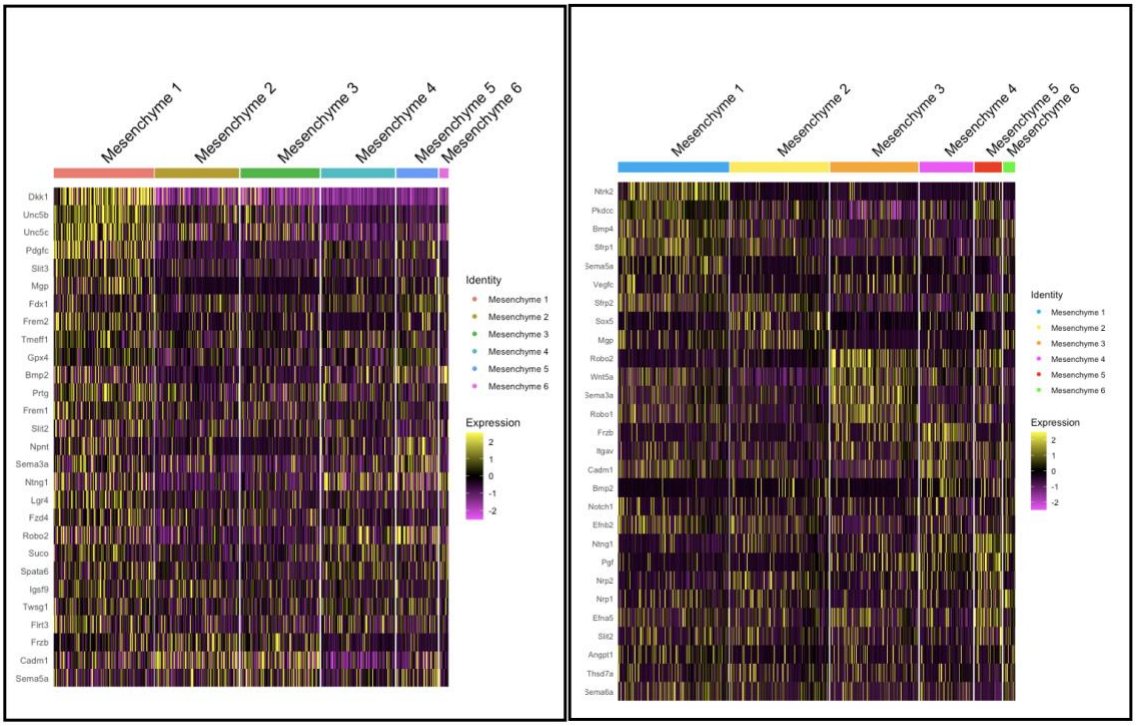

Figure 2.10. Differentially expressed extracellular signals in the NCC mesenchyme at E10.25 (A) and E11.25 (B). Differentially expressed signals were identified by gene ontology terms for “Signal” and “Differentiation.”

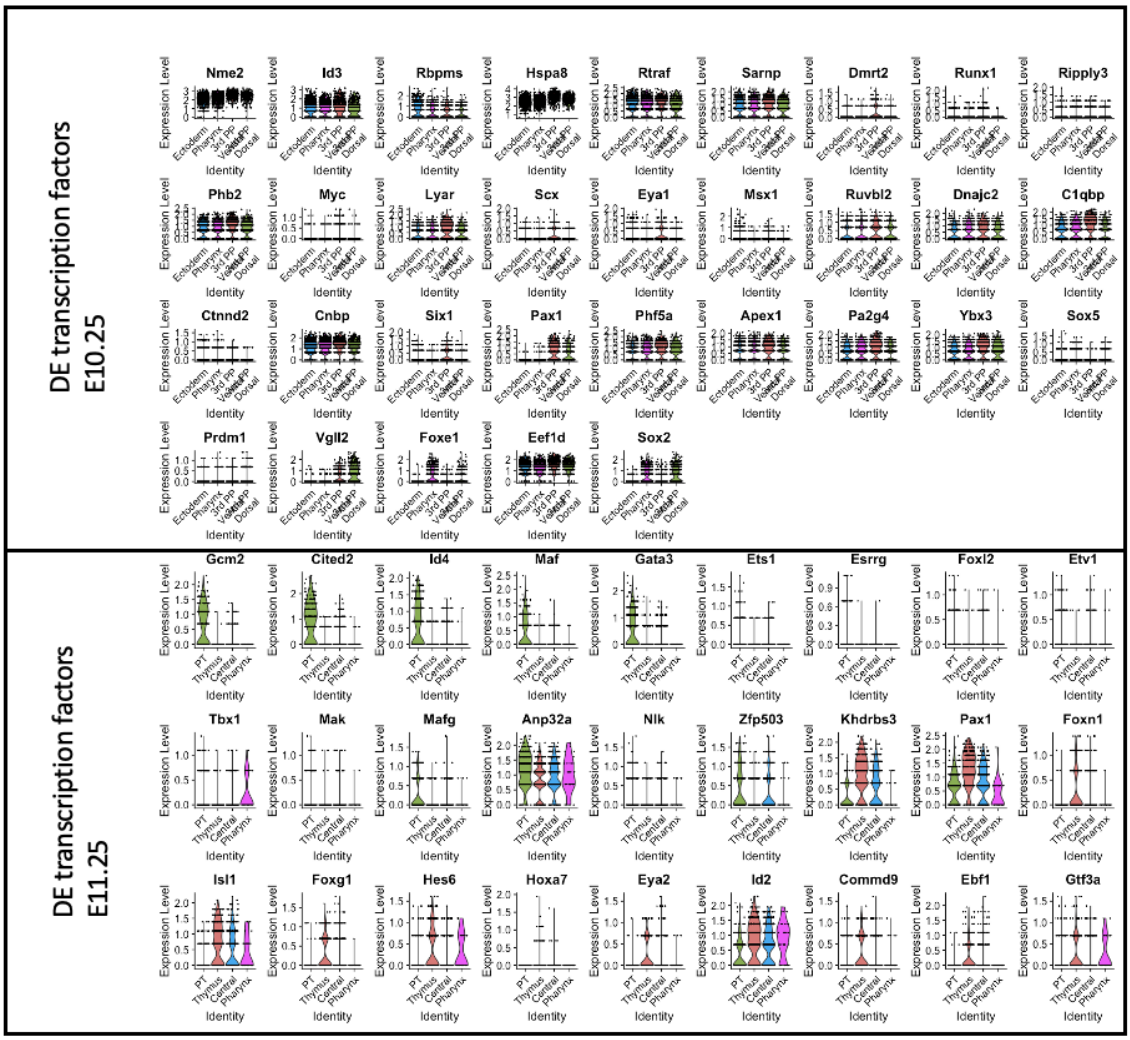

Figure 2.11. Absolute expression of differentially expressed TFs at E10.25 and E11.25. Many differentially expressed transcription factors are highly expressed throughout the 3rd PP or expressed at low levels.

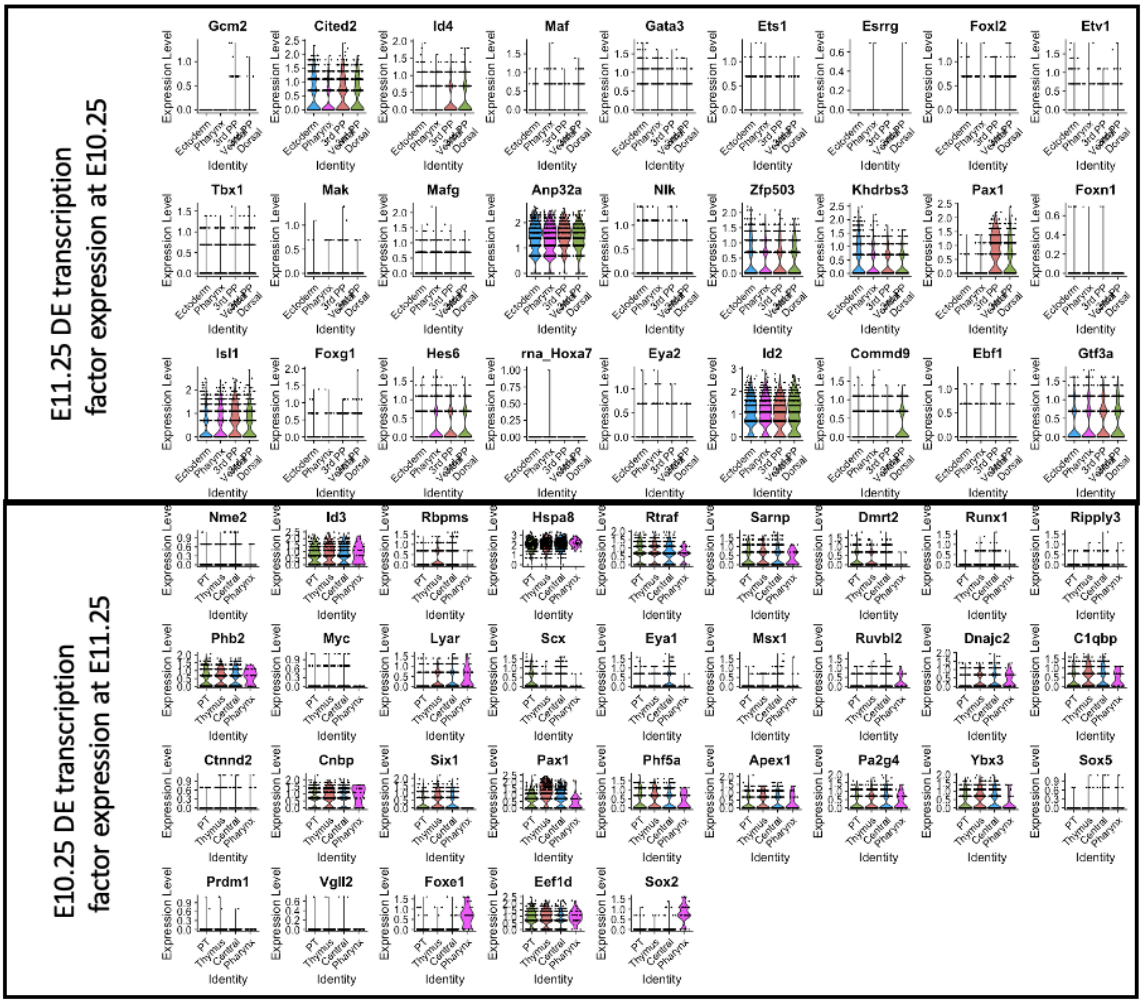

Figure 2.12. Differentially expressed transcription factors identified at E10.25 and E11.25 are ubiquitously expressed or not expressed in the other timepoint. A) Expression of differentially expressed transcription factors identified at E11.25 do not show differential expression at E10.25. B) Differentially expressed transcription factors identified at E10.25 do not show differential expression at E11.25.

Isl1	F	AGCGGCTTTGATTGCGTGCT
	R	TCTGCCATCGCCAGCCTAACA
Id4	F-mutant	ACCCGGAGCTCGCTCTACCGCTTGTCG
	F-WT	AGTCGCCTGCGGAGGCTCGTGCTTACCATC
	R	CCGCCAAGGCTTCTCACCGGGTCAGTGTTG
Foxa2-Cre	F-WT	CTCAAGGGAGCAGTCTCACC
	F-mutant	ATACTATCTAGAGAATAGGAACTTCG
	R	GACTTTTCTGCAACAACAGCA

Table 2.1. Genotyping primers.

CHAPTER 3

CELL CYCLE GATING OF THE SHH PATHWAY RESPONSE

Introduction

Sonic hedgehog signaling

Sonic Hedgehog (SHH) is a major developmental signal driving cell fates in several embryonic tissues. The SHH pathway is complicated and not fully understood. Three transcription factors, GLI1, GLI2, and GLI3 are the effectors of SHH signaling, driving genes important for cell fate specification (Katoh & Katoh, 2009). However, there are many steps between SHH binding to its receptor on a cell and the transcriptional response. The SHH receptor, *patched1 (Ptch1)*, is a negative regulator of the SHH pathway, inhibiting the transmembrane positive regulator of SHH signaling, *Smoothened (Smo)* from entering the cilia (Milenkovic et al., 2015; Taipale et al., 2002). When SHH binds PTCH1, the SHH/PTCH1 complex is internalized and allows SMO to enter and accumulate in the cilia, a step necessary for the SHH response (Milenkovic et al., 2015; Rohatgi et al., 2007; Torroja et al., 2004). Several other genes are implicated in the SHH response, including PKA, GSK3-β, GPR161, and SUFU, all of which mainly act as repressors of the pathway (Bishop et al., 2007; Chen et al., 2011; P. Kogerman et al., 1999; Kotani, 2012; Niewiadomski et al., 2014). During repression, the GLI transcription factors are cleaved into an N-terminal repressor domain (Niewiadomski et al., 2014; Wang & Li, 2006). However, when SHH is present, the GLI transcription factors act as transcriptional activators. In addition to driving genes involved in cell fate specification,

GLI transcription factors drive a common set of genes, such as *Gli1, Ptch1,* and *Hhip*, that are involved in positive and negative feedback loops of SHH signaling, but also serve as readouts of cells responding to SHH (Katoh & Katoh, 2009; Sigulinsky et al., 2021).

Cell cycle regulation of signaling pathways

While many studies involving signaling pathways and the cell cycle have focused on signaling effects on proliferation, especially in cancer cells, few studies have studied the role of the cell cycle in a signaling response. The best example of the cell cycle phase determining a cells response to a signal is in WNT signaling. The ability of a cell to respond to WNT has been shown to be highest in the G2/earlyM phase of the cell cycle. The G2 specific cyclinY/CDK14 phosphorylate the WNT receptor, LRP6, making it most effective in the G2 phase of the cell cycle. Additionally, a *cyclinY* morpholino causes an anteriorization phenotype in *Xenopus*, similar to phenotypes seen in reduced WNT signaling models (Davidson et al., 2009).

Preliminary studies in our lab have shown that proliferating cells have a reduced response to a SMO agonist (SAG) in comparison to that in confluent quiescent cells (Data not shown). However, because cells in an embryo that rely on responding to SHH to drive their cell fate are not quiescent, proliferating cells must respond to SHH at some level. This lead to the hypothesis that proliferating cells respond to SHH differentially throughout the cell cycle, creating an average expression lower than that of quiescent cells. This potential ability to respond to SHH higher in one phase of the cell cycle over the other we refer to as “cell cycle gating.”

In this study, we aim to identify whether proliferating cells respond to SHH differentially in each phase of the cell cycle. We take advantage of the FUCCI cell cycle reporter system to identify which cells are in late M/early G1, late G1, the G1/S transition, S and G2/early M phases (Sakaue-Sawano & Miyawaki, 2014). We show that proliferating NIH-3T3 cells have the highest quantitative response to SHH by qPCR of nascent *Gli1* in cells dosed with a SMO agonist (SAG) in the G2/M phase of the cell cycle. We also show that a higher proportion of NIH-3T3 cells *in vitro* and a higher proportion of neural tube cells *in vivo* respond to SHH with florescent *in situ* hybridization of nascent *Gli1* in the S/G2/M phases. Finally, we show that cells transfected with a constitutively active version of the GLI2 transcription factor (*Gli2ΔN*) activates expression of nascent *Gli1,* and although cells in early G1 (just coming out of mitosis) are less competent to activate *Gli1* expression, cells in the rest of the cell cycle phases are roughly equally competent to induce *Gli1* expression. This suggests that the SHH pathway response is gated to the G2/early M portion of the cell cycle, and that such gating is not due to increased chromatin accessibility in G2/early M, but instead occurs due to differences in Hh signal transduction at a step between SMO and GLI transcription factors.

Methods

Quantitative nascent Gli1 expression in FUCCI NIH-3T3 cells

NIH-3T3 cells expressing FUCCI transgenes were grown at 70% confluency to avoid quiescence. Cells were dosed with 200nM SAG or an equal volume of DMSO as a control for 24 hours. Prior to cell sorting, cells were dosed with 5.6ug/ML of Hoescht-

33532 to identify cells in S phase. Cells were harvested with trypsin and resuspended in FACS buffer (1% FBS, 5mM EDTA and HBSS). Cells were sorted using a MoFlo Astrios EQ into early G1 (colorless), late G1 (red), G1/S transition (Yellow), S (green and low point of Hoechst staining), and G2/M (green and second peak of Hoechst staining). Approximately 200,000 cells from each population was collected. Cells were then centrifuged at 300g for 5 minutes and RNA was collected using an E.Z.N.A Total RNA Kit I. Because nascent *Gli1* qPCR probes do not exclude introns as most qPCR probes do, DNA was digested by incubating RNA with 2 units DNAse1 for 30 minutes at 37 degrees. cDNA was generated using qScript, and qPCR was performed on a 7500 Real Time PCR System (Applied Biosystems) with Syber green reagents. Fold induction was determined using the ddct calculation. qPCR primers were as follows:

Gli1 nascent primer 1: GGTGGCTGATTCTCTTCACTAA

Gli1 nascent primer 2: CATAGGGAGGTGAAGTTCCTTT

Gapdh primer 1: GTGGAGTCATACTGGAACATGTAG

Gapdh primer 2: AATGGTGAAGGTCGGTGTG

Quantitative nascent Gli1 expression in cells transfected with Gli2ΔN

NIH-3T3 FUCCI cells were grown at 70% confluency and transfected with either a *Gli2ΔN* plasmid (Addgene plasmid #17649) or an empty plasmid using a Lipofectamine 3000 kit. Cells were left in the incubator for 24 hours, then sorted using the same

parameters as described above. qPCR on *Gapdh* and nascent *Gli1* was performed as described above.

Quantity of cells responding to SHH in vitro

NIH-3T3 FUCCI cells were grown at 70% in 35mm glass bottom plates and exposed to 200nM SAG for 24 hours. Cells were fixed with 4% PFA for 15 minutes, then washed with PBS. The cell area was outlined with a hydrophobic pen, DAPI was added to the cells for 5 minutes, and the FUCCI signal was imaged using an LSM 710. Fluorescent *in situ* hybridization of the nascent *Gli1* transcript was performed using RNAscope Fluorescent *in situ* hybridization version 2 kit, with a Gli1 intron probe (chr10:127338547-1273412045; ACDBIO Catalog #: 498941-C3; Intron 2). The RNAscope *Gli1* signal was imaged, and the FUCCI image and *Gli1* fluorescent *in situ* hybridization image were overlaid using autofluorescence from the hydrophobic pen ink as a landmark. Cells were counted based on their cell cycle phase as determined by the FUCCI signal an whether they expressed *Gli1* or not.

Results/Conclusions

To determine whether cells respond to SHH differentially throughout the cell cycle, we began by determining the response to a SMO agonist (SAG) in NIH-3T3 cells with the FUCCI cell cycle reporter by qPCR of the nascent *Gli1* transcript. We use the nascent transcript to determine the immediate response to SAG as opposed to a delayed response that may be observed by the accumulation of mature *Gli1* RNA. Cells responded to SHH and SAG differentially throughout the cell cycle. In NIH-3T3 cells

exposed to SAG, the highest expression of nascent *Gli1* transcript was in the G2/M population, followed by cells in S phase (Figure 3.1). This could be explained by either cells in G2/M responding at a higher level to SAG on an individual basis and expressing more *Gli1* per cell, or by a greater proportion of cells in G2/M responding to SAG and expressing *Gli1*.

To determine whether a higher proportion of cells in G2/M respond to SAG or whether cells in G2/M respond at a higher level to SAG, we performed RNAscope fluorescent *in situ* hybridization on the nascent *Gli1* transcript in FUCCI NIH-3T3 cells and determined the proportion of cells expressing *Gli1* in each phase of the cell cycle. This showed that the greatest proportion of cells in S/G2/M phases of the cell cycle express *Gli1* after exposure to SAG (Figure 3.2). One drawback to this experiment is that the FUCCI cell cycle reporter system is unable to identify cells in S compared to cells in G2/M, as both populations express GFP (Sakaue-Sawano & Miyawaki, 2014). When using flow cytometry to isolate cell populations, we were able to use Hoechst staining to separate cells in S phase from those in G2/M. However, using fluorescent *in situ* hybridization we were unable to identify cells in S phase vs. cells in G2/M. Nevertheless, a higher proportion of cells in S/G2/M phases expressed nascent *Gli1* than cells in early or late G1 or the G1/S transition.

To determine whether cells *in vivo* respond to SHH differentially throughout the cell cycle, we used a similar strategy to observe nascent *Gli1* transcripts in neural tube cells of E11.5 embryos that respond to SHH from the adjacent notochord. This showed a similar pattern to that of the NIH-3T3 cells, where a greater proportion of cells in G2/M express nascent *Gli1* transcripts than that of other phases of the cell (Figure 3.3). This

suggests that the cell cycle gating of the SHH response is gated to the G2/M phase of the cell cycle in several cell types and different contexts.

Because proliferating cells undergo large changes in chromatin accessibility as they replicate DNA in S phase and have duplicated DNA in G2, we wanted to determine whether the increased *Gli1* expression in G2/M was due to changes in DNA availability or copy number, or whether the cell cycle gating of the SHH response was upstream of the GLI transcription factors. To do this, we transfected NIH-3T3 cells with a constitutively active GLI allele, *Gli2ΔN*, and determined the response with qPCR of nascent *Gli1*. Although this experiment showed variable nascent *Gli1* expression, the highest level of nascent *Gli1* expression was in late G1, as opposed to S/G2/M phases (Figure 3.4). This suggests that the cell cycle gating of the SHH response is not due to changes in DNA copy number or changes in chromatin accessibility, and instead is likely upstream of the GLI transcription factors.

We show here that the response of cells to SHH is gated by the cell cycle, with the highest response in the G2/M phase. This is similar to the cell cycle gating of the WNT response to G2/M (Davidson et al., 2009). However, the mechanisms of cell cycle gating of the SHH response remain unknown. Further experiments activating the pathway in different points of the pathway through genetic mutants may give insight into which protein is differentially activated during the cell cycle that would lead to the cell cycle gating of the SHH pathway response.

One possibility is that cells in different phases of the cell cycle do or do not have cilia, a structure necessary for the SHH pathway. Studies in other labs have shown that cilia are present throughout the cell cycle (Seeley & Nachury, 2010; Van Kerckvoorde et

al., 2021). In our lab, we showed that cilia are present throughout the cell cycle but are at the highest frequency in G2/M (data not shown). This higher frequency of cilia could explain why a higher proportion of cells respond to SAG in G2/M. Alternatively, the mechanisms of cell cycle gating of the SHH response could be due to direct phosphorylation of SHH pathway components by cyclin/CDK complexes, similar to that seen in WNT signaling (Davidson et al., 2009). In either case, the impacts of cell cycle gating of the SHH pathway response on cell fate specification *in vivo* remains an intriguing question yet to be answered.

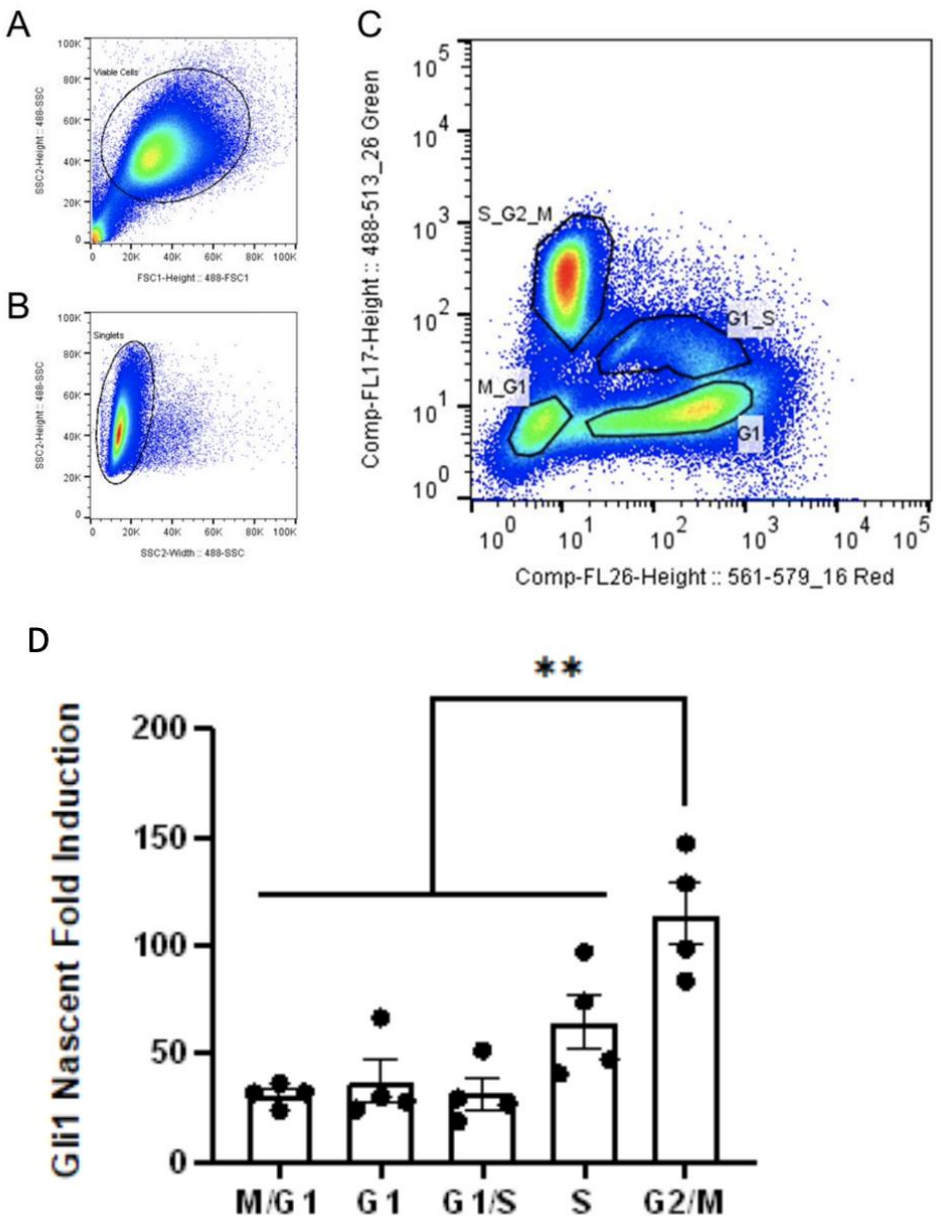

Figure 3.1. Cells in G2/M phase of the cell cycle have the highest level of response to SAG. A-C) Flow cytometry of FUCCI NIH-3T3 cells. D) qPCR of nascent *Gli1* expression in FUCCI NIH-3T3 cells exposed to SAG or DMSO and sorted into each cell cycle phase. Expression induction was calculated using ddct method. Figure adapted from Tyler Miyawaki's thesis.

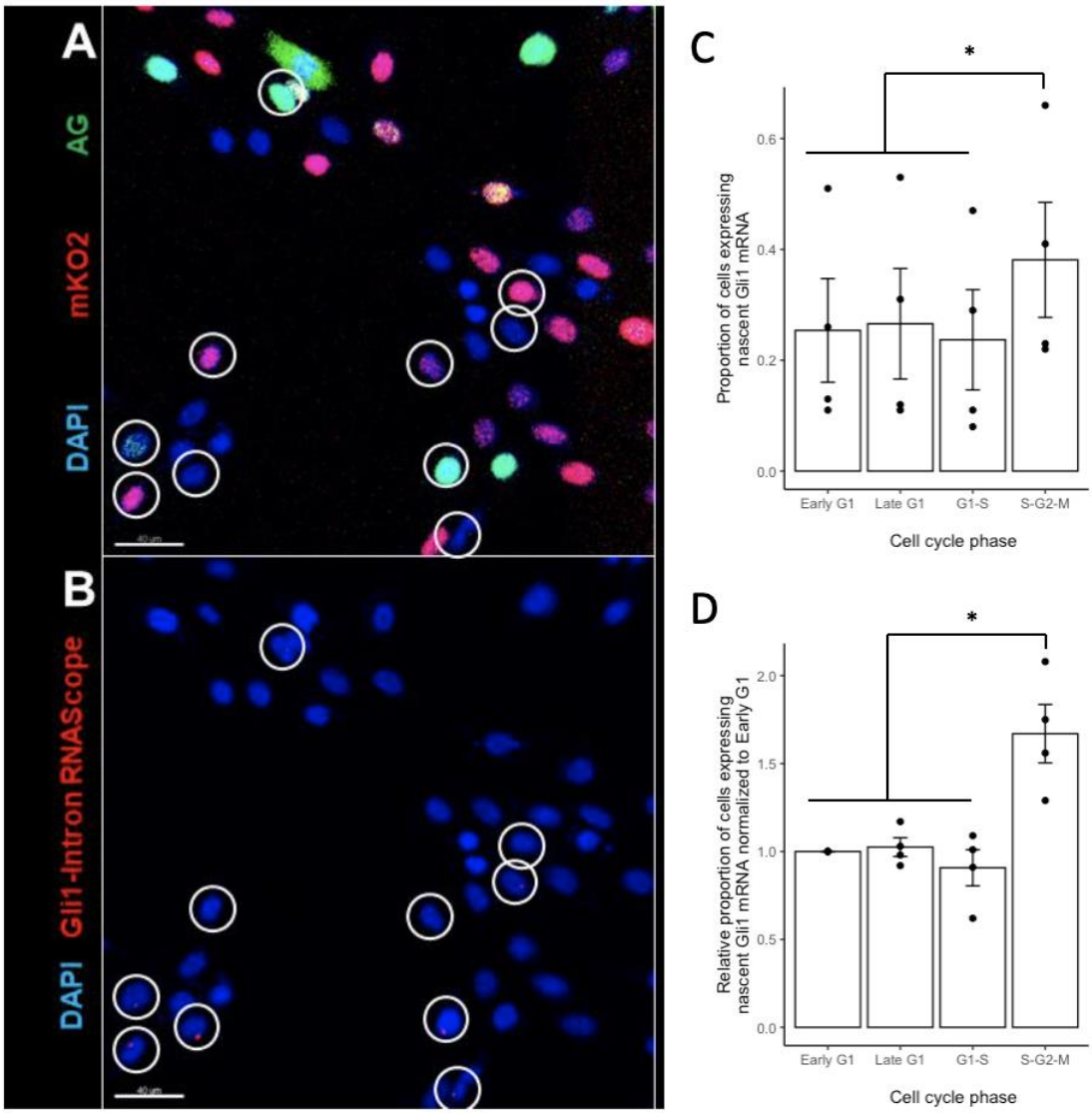

Figure 3.2. NIH-3T3 cells respond to SAG at a higher frequency in G2/M phase of the cell cycle. NIH-3T3 FUCCI cells were quantified based on their cell cycle phase determined by the FUCCI signal (A), and weather they expressed nascent *Gli1* using RNAscope fluorescent *in situ* hybridization (B). The percent of cells in each phase of the cell cycle expressing *Gli1* was quantified (C) and normalized to Early G1 (D). Figure adapted from Tyler Miyawaki's thesis.

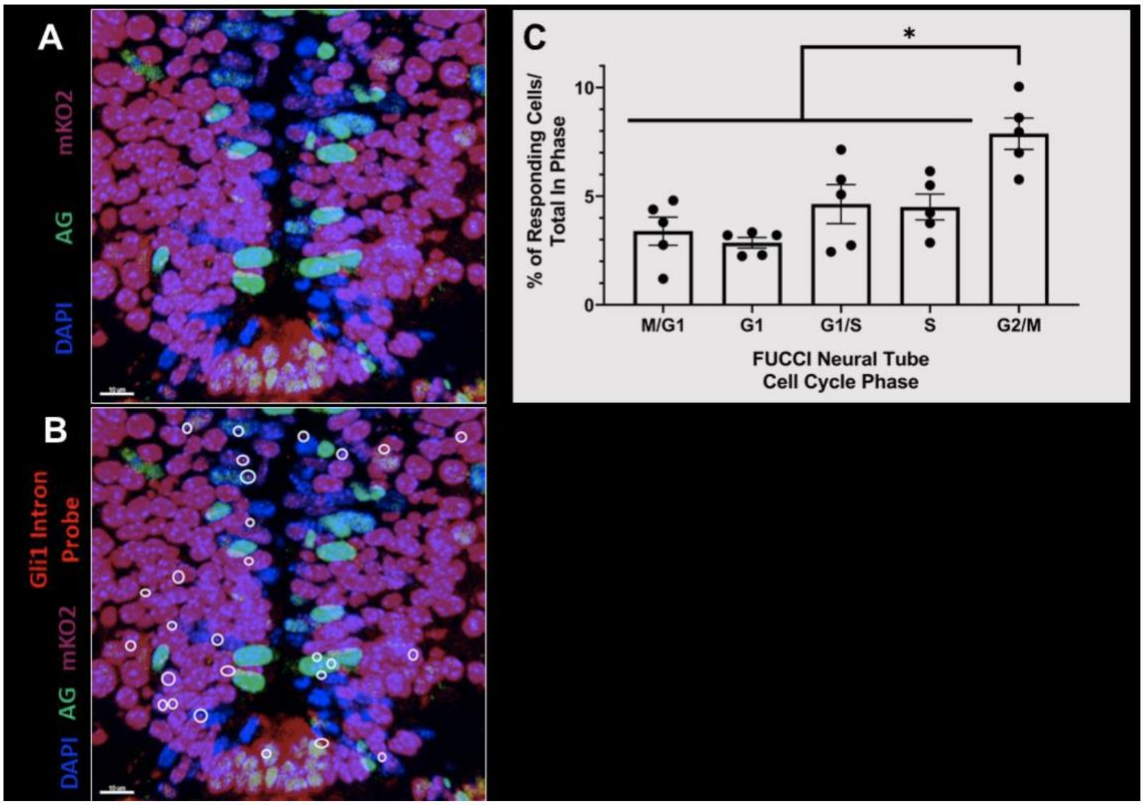

Figure 3.3. Cells *in vivo* respond to endogenous SHH at the highest frequency in G2/M phase of the cell cycle. The cell cycle phase of each cell in the ventral neural tube of E11.5 FUCCI embryo was determined based on the FUCCI signal (A). B) RNAscope florescent *in situ* hybridization of nascent *Gli1* was used to determine which cells are actively responding to SHH endogenously. C) The percent of cells in each cell cycle phase was quantified.

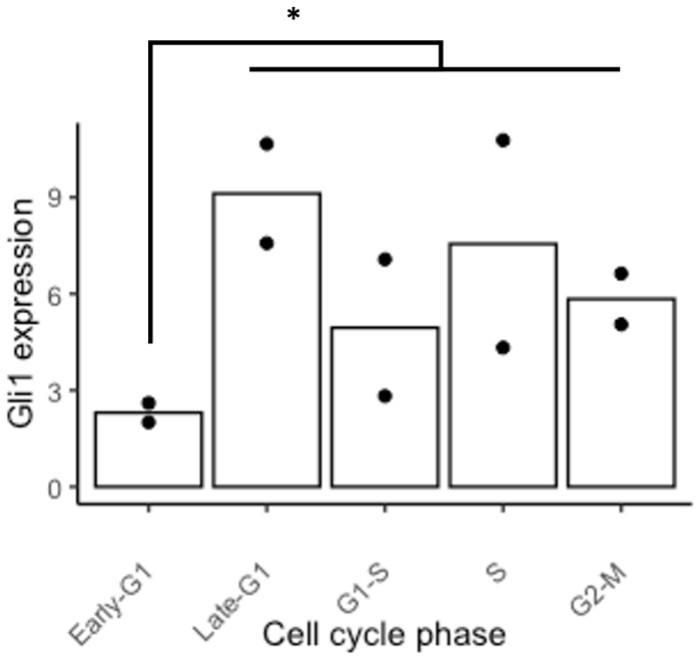

Figure 3.4. NIH-3T3 cells transfected with a constitutively active GLI2 allele do not have the highest *Gli1* expression in G2/M. NIH-3T3 FUCCI cells transfected with *Gli2ΔN* or an empty plasmid were sorted and qPCR was performed on nascent *Gli1* transcripts. Relative expression of nascent *Gli1* was determined using the ddct method. Early G1 express significantly lower *Gli1* than other populations ($p<0.05$).

CHAPTER 4

DISCUSSION AND CONCLUSIONS

The question of how the thymus and parathyroid organs are specified has remained unanswered. Studies have investigated the roles of several transcription factors but have not identified a transcription factor that drives only the thymus or parathyroid cell fate without affecting the entire third pharyngeal pouch. Similarly, previous studies attempting to identify a signal driving either the thymus or parathyroid cell fates have focused on classic developmental signaling proteins such as SHH and BMPs. However, neither of these proteins have been shown to be the sole driver of the thymus or parathyroid cell fates. A major hindrance to previous studies has been the difficulty in identifying candidate genes to test. This hindrance was largely due to a lack of knowledge of the transcriptomes of the developing thymus and parathyroid primordium. In this study, we took advantage of new techniques to both identify new candidate genes involved in the specification of the thymus and the parathyroid and shed new light on genes that have been previously studied.

The transcriptome of the 3rd PP undergoes large changes between E10.25 and E11.25

One interesting result from single cell RNA-seq on the third pharyngeal pouch at E10.25 and E11.25 is the large transcriptional changes that occur over the timeline of specification. This is evident both in the clustering profiles of the two datasets as well as the differently expressed transcription factors at each timepoint. Cells from third

pharyngeal pouch at E10.25 and E11.25 cluster separately based on both cell identity and developmental time. This suggests that the central cells at E11.25 are farther along the specification timeline than at E10.25, even though they do not express the full transcriptomes seen in the “thymus” and “parathyroid” clusters at E11.25.

The second line of evidence showing the large changes in transcriptomes over the timeline of specification is the lack of overlap between the list of differentially expressed transcription factors at E10.25 and E11.25. Only one transcription factor is shared as differentially expressed at both timepoints: *Pax1*. However, *Pax1* is expressed throughout the 3rd PP at both timepoints but shows up as differentially expressed based on the expression level. Additionally, *Pax1* has been previously studied and is involved in 3rd PP identity generally but does not specify the thymus or parathyroid individually (Su et al., 2001; Wallin et al., 1996). All other differentially expressed transcription factors at E11.25 are either not expressed in the 3rd PP at E10.25 or expressed throughout the 3rd PP (and in many cases in the pharynx and surface ectoderm as well). This suggests that the transcriptomes at E11.25 represent those of the already specified thymus and parathyroid, which both upregulate and downregulate many genes. Because *Gcm2* and *Foxn1* play large roles in parathyroid and thymus survival and function, it may be that many of these transcriptional changes are carried out by *Gcm2* and *Foxn1* themselves.

Another insight from scRNA-seq experiments is the heterogeneity of the 3rd PP over time. At E10.25, only two 3rd PP clusters are apparent. However, when viewing marker genes of these clusters, it may be that there is more heterogeneity than observed in the scRNA-seq. Specifically, when observing the expression of *Vgll2*, *Sox2*, and *Gcm2*, one can identify cells that are positive for each marker individually, cells that are

Vgll2/Gcm2 positive, *Sox2/Vgll2* positive, or negative for all three. Although this would suggest there are as many as six cell types in the 3rd PP at E10.25, it is likely that these cells are upregulating and downregulating each gene rapidly, while the rest of the transcriptome does not change enough to create separate clusters in scRNA-seq.

The heterogeneity of the NCC mesenchyme around the 3rd PP undergoes large changes.

The heterogeneity of the mesenchyme similarly changes rapidly. At E10.25, there are three clusters identified in scRNA-seq that are near the 3rd PP. However, two of these are mainly separated by the expression of histone genes and may be the same cell type biologically. Only one mesenchyme cluster appears to be directly adjacent to the 3rd PP, marked by *Barx1*, while the other mesenchymal cell type is slightly separated from the 3rd PP. However, by E11.25, there are four mesenchyme clusters with distinct domains around the 3rd PP on the dorsal-ventral and anterior-posterior axes. This increase in heterogeneity may be explained by external signals driving mesenchymal heterogeneity, or by cell-autonomous transcriptional changes within the mesenchyme. This has been shown in the developing first pharyngeal arch with two genes identified as markers of the E11.25 mesenchyme, *Dlx5* and *Hand2*, where *Dlx5* drives *Hand2* expression, which then inhibits *Dlx5* expression. Around the 3rd PP, both *Dlx5* and *Hand2* are expressed throughout the NCC mesenchyme at E10.25 but are in different domains at E11.25. This is consistent with *Dlx5* driving initial *Hand2* expression, followed by *Hand2* inhibiting *Dlx5* to form separate clusters and increased heterogeneity. However, it is still possible that signals from the pharyngeal endoderm, surface ectoderm and third pharyngeal pouch itself contribute to increased NCC mesenchyme diversity.

WNT signaling pathway is a candidate signal driving 3rd PP cell fates.

Because the NCC mesenchyme lacks diversity at E10.25, and is not necessary for initial 3rd PP cell fate specification as evident from *Pax3splotch/splotch* mutants, it is likely not the main signaling center driving thymus and parathyroid cell fates (Griffith et al., 2009). Therefore, the pharyngeal endoderm, contacting the parathyroid domain, and surface ectoderm, which transiently contacts the thymus domain, are likely the primary sources of signals driving each 3rd PP cell fate. The list of differentially expressed signals from each of these tissues was relatively small and included several known signals. Interestingly, *Shh* was the only positive signal expressed adjacent to the parathyroid domain. This reinforces its role in driving the parathyroid cell fate, but adds additional uncertainty as to why *Gcm2* is still expressed when *Smo* is conditionally knocked out of the 3rd PP, as there is not another apparent signal to compensate for the loss of SHH signaling (Bain et al., 2016; Moore-Scott & Manley, 2005). One possibility is that SHH does not solely act as a positive signal in the 3rd PP driving the parathyroid cell fate, but that it is also necessary to inhibit the thymus cell fate. Previous studies have shown that SHH drives *Tbx1* expression, which in turn inhibits *Foxn1* expression (Bain et al., 2016; Reeh et al., 2014). In this study, we showed that SHH is also sufficient to drive *Sox2* expression. Therefore, it is possible that by driving early *Sox2* expression, SHH inhibits the 3rd PP from specifying into the thymus to allow cells to specify into the parathyroid.

In the surface ectoderm, *Wnt4* and *Wnt6* are expressed at E10.25, when it is in contact with the presumptive thymus domain. The timing of this expression also coincides with the timing of the downregulation of *Sox2* in the ventral domain. If *Sox2* is a negative regulator of cell fates in the 3rd PP, it may be that the lack of *Sox2* in the

ventral domain in combination with the proximity of *Wnt4/6* is necessary for thymus cell fate specification. While the role of WNTs in early specification of the thymus has not been studied, WNT signaling is sufficient to drive *Foxn1* expression in cultured thymus cells post-specification (Balciunaite et al., 2002).

Vgll2 and Sox2 are candidate transcriptomes regulating 3rd PP cell fates

Cell-autonomous specifiers of the thymus and parathyroid cell fates have yet to be identified. By identifying differentially expressed transcription factors in developing domains of the 3rd PP, we hoped to identify candidate specifiers of 3rd PP cell fates. Differentially expressed transcription factors at E11.25 are likely the result of downstream events post-specification, and do not serve as good candidate genes. In fact, the function of two transcription factors differentially expressed at E11.25, *Id4* and *Isl1*, were tested and did not cause a loss of thymus or parathyroid cell fates. Both *Id4* and *Isl1* are expressed throughout the third pharyngeal pouch at E10.5, further weakening them as candidate specifiers of the thymus or parathyroid. Interestingly, *Isl1* was previously identified as a candidate specifier of the thymus cell fate, as it was shown to be expressed exclusively in the ventral 3rd PP at E10.5 using colorimetric *in situ* hybridization (Wei & Condie, 2011). However, using the more sensitive RNAscope fluorescent *in situ* hybridization, as well as data from scRNA-seq, we showed that *Isl1* is expressed throughout the 3rd PP, surface ectoderm and pharyngeal endoderm at E10.5, and is downregulated in the parathyroid by E11.5. Similarly, *Sox2* has previously been described as being absent from the 3rd PP at E9.5, and specific to the dorsal, posterior region at E10.5 using colorimetric *in situ* hybridization (Wei & Condie, 2011). However,

using RNAscope, we were able to confirm this expression pattern at E10.5, but also provide evidence of *Sox2* expression throughout the 3rd PP at E9.5.

Because the transcriptomes of the E11.25 3rd PP likely represent that of the specified thymus and parathyroid, differentially expressed transcription factors at E10.25 are more likely to be the specifiers of the thymus and parathyroid. However, most differentially expressed transcription factors at E10.25 are either expressed throughout the 3rd PP or expressed at very low levels and do not serve as strong candidate genes. Only two had interesting expression profiles: *Sox2* and *Vgll2*. *Sox2* serves as a good inhibitor of 3rd PP cell fates as it precedes *Gcm2* and *Foxn1* expression, but has not been observed to be co-expressed with either gene. This is also consistent with its role in maintaining stem cell pluripotency (Takahashi & Yamanaka, 2006). Additionally, it is expressed in the *Gcm2-Foxn1* negative areas of the 3rd PP in *Sox17-Cre;R26iSmoM2* embryos, which may explain why *Gcm2* expression is not expanded in such embryos.

The only candidate driver of the parathyroid cell fate is *Vgll2*, which has mainly been studied in its role in fast vs. slow twitch muscle fiber differentiation (Hitachi et al., 2019; Honda et al., 2017). In the 3rd PP, *Vgll2* has a dynamic expression pattern. It precedes *Gcm2*, being expressed along with *Sox2* in the dorsal, anterior region of the 3rd PP at E9.5. By E10.5, *Vgll2* is apparent in the dorsal region of the pouch and has overlapping expression with *Gcm2*, but is also in some *Gcm2* negative cells, possibly specifying such cells into the parathyroid before *Gcm2* is expressed. By E11.5, *Vgll2* is not expressed suggesting it may be necessary for initial parathyroid cell fate specification, but not for cell fate maintenance. Supporting the hypothesis that *Vgll2* drives the parathyroid cell fate, it is not expressed in the marker negative region of the 3rd

PP in *Sox17-Cre;R26iSmoM2* embryos. This also suggests that SHH is not sufficient to drive *Vgll2*. However, whether *Shh* is necessary for *Vgll2* expression in the 3rd PP remains unanswered.

Possible thymus cell fate specifiers

One major question asked in this study that was not answered is what transcription factor drives the thymus cell fate. There are two main reasons why such a candidate was not identified. First, it may be that our scRNA-seq timepoints were too far apart. The expression of several other genes show dynamic, transient expression of transcription factors in the third pharyngeal pouch. At E10.25, the thymus domain may have begun its specification as *Sox2* is absent from the region, but the transcription factor driving *Foxn1* and the thymus cell fate may not be expressed yet. By E11.25, when the thymus is specified and *Foxn1* is expressed, the thymus specifier may not be necessary for maintenance of the thymus cell fate and may have already been downregulated. Tighter timepoints of scRNA-seq may identify a transcription factor that is only expressed between E10.25 and E11.25 that would serve as a good candidate of the thymus cell fate specifier.

A second possibility is that the specifier of the thymus cell fate is expressed throughout the 3rd PP but is only active as a protein in the thymus cells. In this case, it would not be identified by our pipeline, as it would not be identified as differentially expressed. One possibility is that the thymus cell fate is specified directly by the effectors of a signaling pathway such as BMP or WNTs. The effectors of both these signaling pathways are frequently expressed ubiquitously, but undergo post-transcriptional

modifications that activate them. In the case of BMP signaling, the binding of BMP to its receptors causes the phosphorylation SMAD1/5/8, which then bind to SMAD4 and translocate to the nucleus to drive target genes (Wang et al., 2014). In canonical WNT signaling, the lack of WNT leads to the degradation of β-catenin. In the presence of WNT, β-catenin is stabilized and translocated to the nucleus, where it forms a complex with the LEF/TCF transcription factors to drive its target genes (Komiya & Habas, 2008). In differentiated thymus cells, *Foxn1* is upregulated directly by the effectors of WNT signaling, as the addition of the protein synthesis inhibitor, cycloheximide, does not inhibit *Foxn1* expression in the presence of WNTs (Balciunaite et al., 2002). It is therefore possible that the thymus cell fate is driven directly by WNT/β-catenin signaling and involves the post-transcriptional modification of proteins that would not be detected at the RNA level in scRNA-seq.

The SHH pathway response is gated to the G2/M phase of the cell cycle

An additional goal of my graduate research was to identify the effect of the cell cycle on the SHH response. While SHH is known to affect the cell cycle, the effect of the cell cycle on the SHH response has not been studied (Kenney & Rowitch, 2000; Komada, 2012). Another common developmental signal, WNT signaling, has been shown to be differentially active in cells depending on their cell cycle phase by the phosphorylation of the WNT receptor by the CyclinY/CDK14 complex (Davidson et al., 2009). Whether other signaling pathway responses are gated by the cell cycle, as well as the role such cell cycle gating may play during development has yet to be identified.

In the case of SHH, we show that cells in the G2/M phase of the cell cycle are most responsive to SHH. There are several lines of evidence supporting this hypothesis. First, NIH-3T3 fibroblasts that express the FUCCI cell cycle reporter were exposed to a SMO agonist (SAG) or a DSMO control and sorted into early G1, late G1, G1/S, S, and G2/M cell cycle populations. qPCR of the nascent *Gli1* transcript, a readout of SHH signaling, showed the highest expression in G2/M. Second, both NIH-3T3 cells and *in vivo* cells marked by FUCCI showed a higher proportion of cells in G2/M phases expressing a nascent *Gli1* transcript as detected by RNAscope fluorescent *in situ* hybridization. Finally, NIH-3T3 FUCCI cells were transfected with a constitutively active *Gli2* allele (*Gli2ΔN*) or a control plasmid, and showed that the pattern of nascent *Gli1* expression being highest in G2/M is lost. This suggests that the differential response of cells in G2/M to SHH is not explained by a change in chromatin structure, and is likely due to differential activation of the SHH pathway between SMO and the GLI transcription factors.

A previous unpublished experiment in the Manley lab showed that the cell cycle affects thymus cell fate specification. Pharyngeal explants cultured with a CDK1 inhibitor that should block the cell cycle at the G2/M transition resulted in a loss of cells expressing *Foxn1* in the central region of the 3rd PP. On the other hand, pharyngeal explants cultured with a CDK4/6 inhibitor that should block cells in G1 did not cause a significant change to *Foxn1* or *Gcm2* expression. This suggests that the thymus cell fate is differentially regulated in different phases of the cell cycle. It is possible that cells in the central region of the 3rd PP that are kept in G2/M with a CDK1 inhibitor are able to respond to both SHH and WNT signals at a higher level. If SHH drives the parathyroid

fate and WNTs drive the thymus cell fates and cells are kept in a cell cycle phase that is more responsive to both these signals, cells may not be able to specify into either the thymus or parathyroid. It is also possible, however, that the addition of CDK inhibitors change cell fates in the 3rd PP through mechanisms not related to SHH or WNT signaling. Further experiments to identify whether such cells are responding to SHH and WNT may shed light on the mechanism of the cell cycle affecting thymus cell fate specification.

Conclusions

While this study was able to take advantage of new technologies to identify possible mechanisms of thymus and parathyroid cell fate specification, the question of how such cell fates are established remains unanswered. Several future directions may be informative however. First, *Vgll2* is the best candidate transcription factor specifying the parathyroid cell fate. To test it however, we would need to look at *Vgll2* mutants to determine if the parathyroid primordium is lost. Additionally, although we show that SHH is not sufficient to drive *Vgll2*, it has not been determined whether it is necessary. Observing *Vgll2* in SHH mutants that lose *Gcm2* expression would answer this question.

Unfortunately, we were unable to identify a candidate thymus cell fate specifier. This could be due to transient expression of such a specifier, or differential activation of its protein. A scRNA-seq experiment between E10.25 and E11.25 may identify a transcription factor with transient expression in the ventral domain prior to *Foxn1* expression that would serve as a good candidate thymus cell fate specifier. If the specifier is expressed throughout the 3rd PP but is only active in the presumptive thymus domain, single cell ATAC-seq with deep sequencing may identify a transcription factor footprint

in open chromatin near *Foxn1*. If the transcription factor with a binding motif matching such a footprint is expressed throughout the third pharyngeal pouch, it may suggest that its protein is only active in the presumptive thymus domain.

Finally, while we were unable to identify a candidate signal driving the parathyroid cell fate other than SHH, we did identify WNT signaling as a candidate driver of the thymus cell fate. Because *Wnt4* and *Wnt6* are expressed in the surface ectoderm and likely are necessary for embryonic viability, a conditional knockout of *Wnt4* and *Wnt6* would be genetically difficult. Other components of the WNT pathway, such as receptors and TCF transcription factors may also have redundancy (van Amerongen & Berns, 2006). The best method to identify whether WNT signaling drives the thymus cell fate is therefore to knockout β-catenin. However, given that β-catenin not only has a role in the transcriptional response of WNT signaling, but also plays a role in cell adhesion, such an experiment may present other difficulties.

This study provided several new candidate genes in the specification of the thymus and parathyroid. While it did not definitively identify the mechanisms of thymus and parathyroid cell fate specification, there are several new future directions to pursue. Using new technologies and new insights from this study, future researchers have a better chance at solving the question as to how the thymus and parathyroid cell fates are specified.

Future directions

There are several future experiments that could improve our knowledge of mechanisms of thymus and parathyroid cell fate specification. First, we believe *Vgll2* is a

good candidate transcription factor driving the parathyroid cell fate. Identifying *Gcm2* and *Foxn1* expression patterns in *Vgll2* mutants will confirm or reject it as a parathyroid cell fate specifier. *Sox2* is a candidate inhibitor of cell fate specification in the third pharyngeal pouch. Observing *Gcm2* and *Foxn1* expression in *Sox2* mutants prior to *Foxn1* and *Gcm2* expression may result in early expression of such markers, possible at the expense of the other. Finally, a more robust knockdown of the WNT signaling pathway in the 3rd PP may inform us of the role of WNTs in thymus cell fate specification.

To address the lack of a candidate thymus cell fate specifier, several experiments may be informative. First, tighter scRNA-seq experiments between E10.25 and E11.25 may identify a transiently expressed transcription factor that would serve as a good candidate thymus cell fate specifier. Second, scATAC-seq on the developing 3rd PP may identify cis-regulatory regions near early thymus markers such as *Foxn1*. Identifying enriched transcription factor motifs or motifs present in open chromatin near *Foxn1* would lead to candidate thymus specifiers. This may also be better to identify transcription factors that are expressed throughout the 3rd PP but only active in the thymus domain. While there are many experiments to do to address the question of how the thymus and parathyroid cell fates are specified, we believe this study has made several important discoveries furthering the field.

REFERENCES

Altaba, A. R. I. (1999). Gli proteins encode context-dependent positive and negative functions: implications for development and disease. *Development*, *126*(14), 3205-3216.

Arnold, J. S., Werling, U., Braunstein, E. M., Liao, J., Nowotschin, S., Edelmann, W., Hebert, J. M., & Morrow, B. E. (2006). Inactivation of Tbx1 in the pharyngeal endoderm results in 22q11DS malformations. *Development*, *133*(5), 977-987. https://doi.org/10.1242/dev.02264

Bafico, A., Gazit, A., Pramila, T., Finch, P. W., Yaniv, A., & Aaronson, S. A. (1999). Interaction of Frizzled Related Protein (FRP) with Wnt Ligands and the Frizzled Receptor Suggests Alternative Mechanisms for FRP Inhibition of Wnt Signaling*. *Journal of Biological Chemistry*, *274*(23), 16180-16187. https://doi.org/https://doi.org/10.1074/jbc.274.23.16180

Bain, V. E., Gordon, J., O'Neil, J. D., Ramos, I., Richie, E. R., & Manley, N. R. (2016). Tissue-specific roles for sonic hedgehog signaling in establishing thymus and parathyroid organ fate. *Development*, *143*(21), 4027-4037. https://doi.org/10.1242/dev.141903

Balciunaite, G., Keller, M. P., Balciunaite, E., Piali, L., Zuklys, S., Mathieu, Y. D., Gill, J., Boyd, R., Sussman, D. J., & Holländer, G. A. (2002). Wnt glycoproteins regulate the expression of FoxN1, the gene defective in nude mice. *Nat Immunol*, *3*(11), 1102-1108. https://doi.org/10.1038/ni850

Barron, F., Woods, C., Kuhn, K., Bishop, J., Howard, M. J., & Clouthier, D. E. (2011). Downregulation of Dlx5 and Dlx6 expression by Hand2 is essential for initiation of tongue morphogenesis. *Development*, *138*(11), 2249-2259. https://doi.org/10.1242/dev.056929

Bishop, G. A., Berbari, N. F., Lewis, J., & Mykytyn, K. (2007). Type III adenylyl cyclase localizes to primary cilia throughout the adult mouse brain. *J Comp Neurol*, *505*(5), 562-571. https://doi.org/10.1002/cne.21510

Boyer, L. A., Lee, T. I., Cole, M. F., Johnstone, S. E., Levine, S. S., Zucker, J. P., Guenther, M. G., Kumar, R. M., Murray, H. L., Jenner, R. G., Gifford, D. K., Melton, D. A., Jaenisch, R., & Young, R. A. (2005). Core Transcriptional Regulatory Circuitry in Human Embryonic Stem Cells. *Cell*, *122*(6), 947-956. https://doi.org/https://doi.org/10.1016/j.cell.2005.08.020

Brehm, A., Miska, E. A., McCance, D. J., Reid, J. L., Bannister, A. J., & Kouzarides, T. (1998). Retinoblastoma protein recruits histone deacetylase to repress transcription. *Nature*, *391*(6667), 597-601. https://doi.org/10.1038/35404

Buchkovich, K., Duffy, L. A., & Harlow, E. (1989). The retinoblastoma protein is phosphorylated during specific phases of the cell cycle. *Cell*, *58*(6), 1097-1105. https://doi.org/10.1016/0092-8674(89)90508-4

Butler, A., Hoffman, P., Smibert, P., Papalexi, E., & Satija, R. (2018). Integrating single-cell transcriptomic data across different conditions, technologies, and species. *Nature Biotechnology*, *36*(5), 411-420. https://doi.org/10.1038/nbt.4096

Cai, C.-L., Liang, X., Shi, Y., Chu, P.-H., Pfaff, S. L., Chen, J., & Evans, S. (2003). Isl1 Identifies a Cardiac Progenitor Population that Proliferates Prior to Differentiation

and Contributes a Majority of Cells to the Heart. *Developmental Cell*, *5*(6), 877-889. https://doi.org/https://doi.org/10.1016/S1534-5807(03)00363-0

Castillo-Azofeifa, D., Seidel, K., Gross, L., Golden, E. J., Jacquez, B., Klein, O. D., & Barlow, L. A. (2018). SOX2 regulation by hedgehog signaling controls adult lingual epithelium homeostasis. *Development*, *145*(14). https://doi.org/10.1242/dev.164889

Chen, Y., Yue, S., Xie, L., Pu, X. H., Jin, T., & Cheng, S. Y. (2011). Dual Phosphorylation of suppressor of fused (Sufu) by PKA and GSK3beta regulates its stability and localization in the primary cilium. *J Biol Chem*, *286*(15), 13502-13511. https://doi.org/10.1074/jbc.M110.217604

Ching, S. T., Infante, C. R., Du, W., Sharir, A., Park, S., Menke, D. B., & Klein, O. D. (2018). Isl1 mediates mesenchymal expansion in the developing external genitalia via regulation of Bmp4, Fgf10 and Wnt5a. *Hum Mol Genet*, *27*(1), 107-119. https://doi.org/10.1093/hmg/ddx388

Chisaka, O., & Capecchi, M. R. (1991). Regionally restricted developmental defects resulting from targeted disruption of the mouse homeobox gene hox-1.5. *Nature*, *350*(6318), 473-479. https://doi.org/10.1038/350473a0

Chojnowski, J. L., Masuda, K., Trau, H. A., Thomas, K., Capecchi, M., & Manley, N. R. (2014). Multiple roles for HOXA3 in regulating thymus and parathyroid differentiation and morphogenesis in mouse. *Development*, *141*(19), 3697-3708. https://doi.org/10.1242/dev.110833

Cordier, A. C., & Haumont, S. M. (1980). Development of thymus, parathyroids, and ultimo-branchial bodies in NMRI and nude mice. *Am J Anat*, *157*(3), 227-263. https://doi.org/10.1002/aja.1001570303

Cordier, A. C., & Heremans, J. F. (1975). Nude mouse embryo: ectodermal nature of the primordial thymic defect. *Scand J Immunol*, *4*(2), 193-196. https://doi.org/10.1111/j.1365-3083.1975.tb02616.x

Davidson, G., Shen, J., Huang, Y. L., Su, Y., Karaulanov, E., Bartscherer, K., Hassler, C., Stannek, P., Boutros, M., & Niehrs, C. (2009). Cell cycle control of wnt receptor activation. *Dev Cell*, *17*(6), 788-799. https://doi.org/10.1016/j.devcel.2009.11.006

Fortunato, S. A. V., Leininger, S., & Adamska, M. (2014). Evolution of the Pax-Six-Eya-Dach network: the calcisponge case study. *EvoDevo*, *5*(1), 23. https://doi.org/10.1186/2041-9139-5-23

Foster, K. E., Gordon, J., Cardenas, K., Veiga-Fernandes, H., Makinen, T., Grigorieva, E., Wilkinson, D. G., Blackburn, C. C., Richie, E., Manley, N. R., Adams, R. H., Kioussis, D., & Coles, M. C. (2010). EphB–ephrin-B2 interactions are required for thymus migration during organogenesis. *Proceedings of the National Academy of Sciences*, *107*(30), 13414-13419. https://doi.org/10.1073/pnas.1003747107

Furushima, K., Yamamoto, A., Nagano, T., Shibata, M., Miyachi, H., Abe, T., Ohshima, N., Kiyonari, H., & Aizawa, S. (2007). Mouse homologues of Shisa antagonistic to Wnt and Fgf signalings. *Developmental Biology*, *306*(2), 480-492. https://doi.org/https://doi.org/10.1016/j.ydbio.2007.03.028

Gardiner, J. R., Jackson, A. L., Gordon, J., Lickert, H., Manley, N. R., & Basson, M. A. (2012). Localised inhibition of FGF signalling in the third pharyngeal pouch is

required for normal thymus and parathyroid organogenesis. *Development*, *139*(18), 3456-3466. https://doi.org/10.1242/dev.079400

Garfin, P. M., Min, D., Bryson, J. L., Serwold, T., Edris, B., Blackburn, C. C., Richie, E. R., Weinberg, K. I., Manley, N. R., Sage, J., & Viatour, P. (2013). Inactivation of the RB family prevents thymus involution and promotes thymic function by direct control of Foxn1 expression. *J Exp Med*, *210*(6), 1087-1097. https://doi.org/10.1084/jem.20121716

Gaunt, S. J. (1987). Homoeobox gene Hox-1.5 expression in mouse embryos: earliest detection by in situ hybridization is during gastrulation. *Development*, *101*(1), 51-60.

Gaunt, S. J. (1988). Mouse homeobox gene transcripts occupy different but overlapping domains in embryonic germ layers and organs: a comparison of Hox-3.1 and Hox-1.5. *Development*, *103*(1), 135-144. https://doi.org/10.1242/dev.103.1.135

Girard, F., Strausfeld, U., Fernandez, A., & Lamb, N. J. (1991). Cyclin A is required for the onset of DNA replication in mammalian fibroblasts. *Cell*, *67*(6), 1169-1179. https://doi.org/10.1016/0092-8674(91)90293-8

Gordon, J., Bennetta, A. R., Blackburn, C. C., & Manley, N. R. (2001). Gcm2 and Foxn1 mark early parathyroid- and thymus-specific domains in the developing third pharyngeal pouch. *Mechanisms of Development*, *103*, 141-143.

Gordon, J., Patel, S. R., Mishina, Y., & Manley, N. R. (2010). Evidence for an early role for BMP4 signaling in thymus and parathyroid morphogenesis. *Dev Biol*, *339*(1), 141-154. https://doi.org/10.1016/j.ydbio.2009.12.026

Gordon, J., Wilson, V. A., Blair, N. F., Sheridan, J., Farley, A., Wilson, L., Manley, N. R., & Blackburn, C. C. (2004). Functional evidence for a single endodermal origin for the thymic epithelium. *Nature Immunology*, *5*(5), 546-553. https://doi.org/10.1038/ni1064

Griffith, A. V., Cardenas, K., Carter, C., Gordon, J., Iberg, A., Engleka, K., Epstein, J. A., Manley, N. R., & Richie, E. R. (2009). Increased thymus- and decreased parathyroid-fated organ domains in Splotch mutant embryos. *Dev Biol*, *327*(1), 216-227. https://doi.org/10.1016/j.ydbio.2008.12.019

Grigorieva, I. V., Mirczuk, S., Gaynor, K. U., Nesbit, M. A., Grigorieva, E. F., Wei, Q., Ali, A., Fairclough, R. J., Stacey, J. M., Stechman, M. J., Mihai, R., Kurek, D., Fraser, W. D., Hough, T., Condie, B. G., Manley, N., Grosveld, F., & Thakker, R. V. (2010). Gata3-deficient mice develop parathyroid abnormalities due to dysregulation of the parathyroid-specific transcription factor Gcm2. *The Journal of Clinical Investigation*, *120*(6), 2144-2155. https://doi.org/10.1172/JCI42021

Günther, T., Chen, Z.-F., Kim, J., Priemel, M., Rueger, J. M., Amling, M., Moseley, J. M., Martin, T. J., Anderson, D. J., & Karsenty, G. (2000). Genetic ablation of parathyroid glands reveals another source of parathyroid hormone. *Nature*, *406*(6792), 199-203. https://doi.org/10.1038/35018111

Hao, Y., Hao, S., Andersen-Nissen, E., Mauck, W. M., 3rd, Zheng, S., Butler, A., Lee, M. J., Wilk, A. J., Darby, C., Zager, M., Hoffman, P., Stoeckius, M., Papalexi, E., Mimitou, E. P., Jain, J., Srivastava, A., Stuart, T., Fleming, L. M., Yeung, B., . . . Satija, R. (2021). Integrated analysis of multimodal single-cell data. *Cell*, *184*(13), 3573-3587.e3529. https://doi.org/10.1016/j.cell.2021.04.048

Hasten, E., & Morrow, B. E. (2019). Tbx1 and Foxi3 genetically interact in the pharyngeal pouch endoderm in a mouse model for 22q11.2 deletion syndrome. *PLOS Genetics*, *15*(8), e1008301. https://doi.org/10.1371/journal.pgen.1008301

Hitachi, K., Inagaki, H., Kurahashi, H., Okada, H., Tsuchida, K., & Honda, M. (2019). Deficiency of Vgll2 Gene Alters the Gene Expression Profiling of Skeletal Muscle Subjected to Mechanical Overload [Data Report]. *Frontiers in Sports and Active Living*, *1*. https://doi.org/10.3389/fspor.2019.00041

Honda, M., Hidaka, K., Fukada, S.-i., Sugawa, R., Shirai, M., Ikawa, M., & Morisaki, T. (2017). Vestigial-like 2 contributes to normal muscle fiber type distribution in mice. *Scientific Reports*, *7*(1), 7168. https://doi.org/10.1038/s41598-017-07149-0

Hou, P.-S., hAilín, D. Ó., Vogel, T., & Hanashima, C. (2020). Transcription and Beyond: Delineating FOXG1 Function in Cortical Development and Disorders [Review]. *Frontiers in Cellular Neuroscience*, *14*. https://doi.org/10.3389/fncel.2020.00035

i Altaba, A. R., Mas, C., & Stecca, B. (2007). The Gli code: an information nexus regulating cell fate, stemness and cancer. *Trends in cell biology*, *17*(9), 438-447.

Jamali, M., Karamboulas, C., Rogerson, P. J., & Skerjanc, I. S. (2001). BMP signaling regulates Nkx2-5 activity during cardiomyogenesis. *FEBS Lett*, *509*(1), 126-130. https://doi.org/10.1016/s0014-5793(01)03151-9

Jerome, L. A., & Papaioannou, V. E. (2001). DiGeorge syndrome phenotype in mice mutant for the T-box gene, Tbx1. *Nature Genetics*, *27*(3), 286-291. https://doi.org/10.1038/85845

Kaestner, K. H., Kno¨chel, W., & Martı´nez, D. E. (2000). Unified nomenclature for the winged helix/forkhead transcription factors. *Genes & Development*, *14*, 142–146.

Kato, J., Matsushime, H., Hiebert, S. W., Ewen, M. E., & Sherr, C. J. (1993). Direct binding of cyclin D to the retinoblastoma gene product (pRb) and pRb phosphorylation by the cyclin D-dependent kinase CDK4. *Genes Dev*, *7*(3), 331-342. https://doi.org/10.1101/gad.7.3.331

Katoh, Y., & Katoh, M. (2009). Hedgehog target genes: mechanisms of carcinogenesis induced by aberrant hedgehog signaling activation. *Curr Mol Med*, *9*(7), 873-886. https://doi.org/10.2174/156652409789105570

Kawakami, Y., Marti, M., Kawakami, H., Itou, J., Quach, T., Johnson, A., Sahara, S., O'Leary, D. D. M., Nakagawa, Y., Lewandoski, M., Pfaff, S., Evans, S. M., & Belmonte, J. C. I. (2011). Islet1-mediated activation of the β-catenin pathway is necessary for hindlimb initiation in mice. *Development*, *138*(20), 4465-4473. https://doi.org/10.1242/dev.065359

Kenney, A. M., & Rowitch, D. H. (2000). Sonic hedgehog promotes G(1) cyclin expression and sustained cell cycle progression in mammalian neuronal precursors. *Molecular and Cellular Biology*, *20*(23), 9055-9067. https://doi.org/10.1128/MCB.20.23.9055-9067.2000

King, R. W., Jackson, P. K., & Kirschner, M. W. (1994). Mitosis in transition. *Cell*, *79*(4), 563-571. https://doi.org/10.1016/0092-8674(94)90542-8

Kogerman, P., Grimm, T., Kogerman, L., Krause, D., Undén, A. B., Sandstedt, B., Toftgård, R., & Zaphiropoulos, P. G. (1999). Mammalian suppressor-of-fused modulates nuclear-cytoplasmic shuttling of Gli-1. *Nat Cell Biol*, *1*(5), 312-319. https://doi.org/10.1038/13031

Kogerman, P., Grimm, T., Kogerman, L., Krause, D., Undén, A. B., Sandstedt, B., Toftgård, R., & Zaphiropoulos, P. G. (1999). Mammalian Suppressor-of-Fused modulates nuclear–cytoplasmic shuttling of GLI-1. *Nature cell biology*, *1*(5), 312-319.

Komada, M. (2012). Sonic hedgehog signaling coordinates the proliferation and differentiation of neural stem/progenitor cells by regulating cell cycle kinetics during development of the neocortex. *Congenital Anomalies*, *52*(2), 72-77. https://doi.org/https://doi.org/10.1111/j.1741-4520.2012.00368.x

Komiya, Y., & Habas, R. (2008). Wnt signal transduction pathways. *Organogenesis*, *4*(2), 68-75.

Kotani, T. (2012). Protein kinase A activity and Hedgehog signaling pathway. *Vitam Horm*, *88*, 273-291. https://doi.org/10.1016/b978-0-12-394622-5.00012-2

Ladher, R. K., Church, V. L., Allen, S., Robson, L., Abdelfattah, A., Brown, N. A., Hattersley, G., Rosen, V., Luyten, F. P., Dale, L., & Francis-West, P. H. (2000). Cloning and expression of the Wnt antagonists Sfrp-2 and Frzb during chick development. *Dev Biol*, *218*(2), 183-198. https://doi.org/10.1006/dbio.1999.9586

Liang, C. J., Wang, Z. W., Chang, Y. W., Lee, K. C., Lin, W. H., & Lee, J. L. (2019). SFRPs Are Biphasic Modulators of Wnt-Signaling-Elicited Cancer Stem Cell Properties beyond Extracellular Control. *Cell Rep*, *28*(6), 1511-1525 e1515. https://doi.org/10.1016/j.celrep.2019.07.023

Lind, E. F., Prockop, S. E., Porritt, H. E., & Petrie, H. T. (2001). Mapping precursor movement through the postnatal thymus reveals specific microenvironments

supporting defined stages of early lymphoid development. *The Journal of Experimental Medicine*, *194*(2), 127-134. https://doi.org/10.1084/jem.194.2.127

Lindsay, E. A., Vitelli, F., Su, H., Morishima, M., Huynh, T., Pramparo, T., Jurecic, V., Ogunrinu, G., Sutherland, H. F., Scambler, P. J., Bradley, A., & Baldini, A. (2001). Tbx1 haploinsufficiency in the DiGeorge syndrome region causes aortic arch defects in mice. *Nature*, *410*(6824), 97-101. https://doi.org/10.1038/35065105

Liu, Z., Yu, S., & Manley, N. R. (2007). Gcm2 is required for the differentiation and survival of parathyroid precursor cells in the parathyroid/thymus primordia. *Dev Biol*, *305*(1), 333-346. https://doi.org/10.1016/j.ydbio.2007.02.014

Lyons, I., Parsons, L. M., Hartley, L., Li, R., Andrews, J. E., Robb, L., & Harvey, R. P. (1995). Myogenic and morphogenetic defects in the heart tubes of murine embryos lacking the homeo box gene Nkx2-5. *Genes Dev*, *9*(13), 1654-1666. https://doi.org/10.1101/gad.9.13.1654

Manley, N. R., & Capecchi, M. R. (1995). The role of Hoxa-3 in mouse thymus and thyroid development. *Development*, *121*(7), 1989-2003. https://doi.org/10.1242/dev.121.7.1989

Merscher, S., Funke, B., Epstein, J. A., Heyer, J., Puech, A., Lu, M. M., Xavier, R. J., Demay, M. B., Russell, R. G., Factor, S., Tokooya, K., Jore, B. S., Lopez, M., Pandita, R. K., Lia, M., Carrion, D., Xu, H., Schorle, H., Kobler, J. B., . . . Kucherlapati, R. (2001). TBX1 Is Responsible for Cardiovascular Defects in Velo-Cardio-Facial/DiGeorge Syndrome. *Cell*, *104*(4), 619-629. https://doi.org/10.1016/S0092-8674(01)00247-1

Milenkovic, L., Weiss, L. E., Yoon, J., Roth, T. L., Su, Y. S., Sahl, S. J., Scott, M. P., & Moerner, W. E. (2015). Single-molecule imaging of Hedgehog pathway protein Smoothened in primary cilia reveals binding events regulated by Patched1. *Proc Natl Acad Sci U S A*, *112*(27), 8320-8325. https://doi.org/10.1073/pnas.1510094112

Miller, J. F. A. P. (1965). Effect of Thymectomy in Adult Mice on Immunological Responsiveness. *Nature*, *208*(5017), 1337-1338. https://doi.org/10.1038/2081337a0

Miller, J. F. A. P., & Mitchell, G. F. (1967). The Thymus and the Precursors of Antigen Reactive Cells. *Nature*, *216*(5116), 659-663. https://doi.org/10.1038/216659a0

Mirotsou, M., Zhang, Z., Deb, A., Zhang, L., Gnecchi, M., Noiseux, N., Mu, H., Pachori, A., & Dzau, V. (2007). Secreted frizzled related protein 2 (Sfrp2) is the key Akt-mesenchymal stem cell-released paracrine factor mediating myocardial survival and repair. *Proceedings of the National Academy of Sciences*, *104*(5), 1643-1648. https://doi.org/doi:10.1073/pnas.0610024104

Moore-Scott, B. A., & Manley, N. R. (2005). Differential expression of Sonic hedgehog along the anterior-posterior axis regulates patterning of pharyngeal pouch endoderm and pharyngeal endoderm-derived organs. *Dev Biol*, *278*(2), 323-335. https://doi.org/10.1016/j.ydbio.2004.10.027

Narkis, G., Tzchori, I., Cohen, T., Holtz, A., Wier, E., & Westphal, H. (2012). Isl1 and Ldb co-regulators of transcription are essential early determinants of mouse limb development. *Dev Dyn*, *241*(4), 787-791. https://doi.org/10.1002/dvdy.23761

Nehls, M., Kyewski, B., Messerle, M., Waldschutz, R., Schuddekopf, K., Smith, A. J. H., & Boehm, T. (1996). Two Genetically Seperable Steps in the Differentiation of Thymic Epithelium. *Science, 272*, 886-889.

Nestorowa, S., Hamey, F. K., Pijuan Sala, B., Diamanti, E., Shepherd, M., Laurenti, E., Wilson, N. K., Kent, D. G., & Göttgens, B. (2016). A single-cell resolution map of mouse hematopoietic stem and progenitor cell differentiation. *Blood, 128*(8), e20-e31. https://doi.org/10.1182/blood-2016-05-716480

Neves, H., Dupin, E., Parreira, L., & Le Douarin, N. M. (2012). Modulation of Bmp4 signalling in the epithelial-mesenchymal interactions that take place in early thymus and parathyroid development in avian embryos. *Dev Biol*, *361*(2), 208-219. https://doi.org/10.1016/j.ydbio.2011.10.022

Niewiadomski, P., Kong, J. H., Ahrends, R., Ma, Y., Humke, E. W., Khan, S., Teruel, M. N., Novitch, B. G., & Rohatgi, R. (2014). Gli protein activity is controlled by multisite phosphorylation in vertebrate Hedgehog signaling. *Cell Rep*, *6*(1), 168-181. https://doi.org/10.1016/j.celrep.2013.12.003

Ohtani, K., DeGregori, J., & Nevins, J. R. (1995). Regulation of the cyclin E gene by transcription factor E2F1. *Proc Natl Acad Sci U S A*, *92*(26), 12146-12150. https://doi.org/10.1073/pnas.92.26.12146

Ohtsubo, M., Theodoras, A. M., Schumacher, J., Roberts, J. M., & Pagano, M. (1995). Human cyclin E, a nuclear protein essential for the G1-to-S phase transition. *Mol Cell Biol*, *15*(5), 2612-2624. https://doi.org/10.1128/mcb.15.5.2612

Olmeda, D., Castel, S., Vilaró, S., & Cano, A. (2003). Beta-catenin regulation during the cell cycle: implications in G2/M and apoptosis. *Mol Biol Cell*, *14*(7), 2844-2860. https://doi.org/10.1091/mbc.e03-01-0865

Pantelouris, E. M. (1968). Absence of Thymus in a Mouse Mutant. *Nature*, *217*(5126), 370-371. https://doi.org/10.1038/217370a0

Patel, S. R., Gordon, J., Mahbub, F., Blackburn, C. C., & Manley, N. R. (2006). Bmp4 and Noggin expression during early thymus and parathyroid organogenesis. *Gene Expr Patterns*, *6*(8), 794-799. https://doi.org/10.1016/j.modgep.2006.01.011

Pauklin, S., Madrigal, P., Bertero, A., & Vallier, L. (2016). Initiation of stem cell differentiation involves cell cycle-dependent regulation of developmental genes by Cyclin D. *Genes & Development*, *30*(4), 421-433. https://doi.org/10.1101/gad.271452.115

Pauklin, S., & Vallier, L. (2013). The cell-cycle state of stem cells determines cell fate propensity. *Cell*, *155*(1), 135-147. https://doi.org/10.1016/j.cell.2013.08.031

Peters, H., Neubuser, A., Kratochwil, K., & Balling, R. (1998). *Pax9*-deficient mice lack pharyngeal pouch derivatives and teeth and exhibit craniofacial and limb abnormalities. *Genes & Development*, *12*, 2735-2747.

Pongracz, J., Hare, K., Harman, B., Anderson, G., & Jenkinson, E. J. (2003). Thymic epithelial cells provide Wnt signals to developing thymocytes. *European Journal of Immunology*, *33*(7), 1949-1956. https://doi.org/https://doi.org/10.1002/eji.200323564

Reeh, K. A., Cardenas, K. T., Bain, V. E., Liu, Z., Laurent, M., Manley, N. R., & Richie, E. R. (2014). Ectopic TBX1 suppresses thymic epithelial cell differentiation and

proliferation during thymus organogenesis. *Development*, *141*(15), 2950-2958. https://doi.org/10.1242/dev.111641

Rohatgi, R., Milenkovic, L., & Scott, M. P. (2007). Patched1 regulates hedgehog signaling at the primary cilium. *Science*, *317*(5836), 372-376. https://doi.org/10.1126/science.1139740

Sakaue-Sawano, A., & Miyawaki, A. (2014). Visualizing spatiotemporal dynamics of multicellular cell-cycle progressions with fucci technology. *Cold Spring Harb Protoc*, *2014*(5). https://doi.org/10.1101/pdb.prot080408

Sasaki, H., Nishizaki, Y., Hui, C., Nakafuku, M., & Kondoh, H. (1999). Regulation of Gli2 and Gli3 activities by an amino-terminal repression domain: implication of Gli2 and Gli3 as primary mediators of Shh signaling. *Development*, *126*(17), 3915-3924. https://doi.org/10.1242/dev.126.17.3915

Satija, R., Farrell, J. A., Gennert, D., Schier, A. F., & Regev, A. (2015). Spatial reconstruction of single-cell gene expression data. *Nature Biotechnology*, *33*(5), 495-502. https://doi.org/10.1038/nbt.3192

Seeley, E. S., & Nachury, M. V. (2010). The perennial organelle: assembly and disassembly of the primary cilium. *J Cell Sci*, *123*(Pt 4), 511-518. https://doi.org/10.1242/jcs.061093

Segre, J. A., Nemhauser, J. L., Taylor, B. A., Nadeau, J. H., & Lander, E. S. (1995). Positional Cloning of the nude Locus: Genetic, Physical, and Transcription Maps of the Region and Mutations in the Mouse and Rat. *Genomics*, *28*(3), 549-559. https://doi.org/https://doi.org/10.1006/geno.1995.1187

Sherr, C. J. (1994). G1 phase progression: cycling on cue. *Cell*, *79*(4), 551-555. https://doi.org/10.1016/0092-8674(94)90540-1

Sigulinsky, C. L., Li, X., & Levine, E. M. (2021). Expression of Sonic Hedgehog and pathway components in the embryonic mouse head: anatomical relationships between regulators of positive and negative feedback. *BMC Research Notes*, *14*(1), 300. https://doi.org/10.1186/s13104-021-05714-5

Stuart, T., Butler, A., Hoffman, P., Hafemeister, C., Papalexi, E., Mauck, W. M., 3rd, Hao, Y., Stoeckius, M., Smibert, P., & Satija, R. (2019). Comprehensive Integration of Single-Cell Data. *Cell*, *177*(7), 1888-1902.e1821. https://doi.org/10.1016/j.cell.2019.05.031

Su, D.-m., Ellis, S., Napier, A., Lee, K., & Manley, N. R. (2001). Hoxa3 and Pax1 Regulate Epithelial Cell Death and Proliferation during Thymus and Parathyroid Organogenesis. *Developmental Biology*, *236*(2), 316-329. https://doi.org/https://doi.org/10.1006/dbio.2001.0342

Svärd, J., Heby-Henricson, K., Persson-Lek, M., Rozell, B., Lauth, M., Bergström, A., Ericson, J., Toftgård, R., & Teglund, S. (2006). Genetic elimination of Suppressor of fused reveals an essential repressor function in the mammalian Hedgehog signaling pathway. *Dev Cell*, *10*(2), 187-197. https://doi.org/10.1016/j.devcel.2005.12.013

Swann, J. B., Happe, C., & Boehm, T. (2017). Elevated levels of Wnt signaling disrupt thymus morphogenesis and function. *Scientific Reports*, *7*(1), 785. https://doi.org/10.1038/s41598-017-00842-0

Taipale, J., Cooper, M. K., Maiti, T., & Beachy, P. A. (2002). Patched acts catalytically to suppress the activity of Smoothened. *Nature*, *418*(6900), 892-897. https://doi.org/10.1038/nature00989

Takahashi, K., & Yamanaka, S. (2006). Induction of Pluripotent Stem Cells from Mouse Embryonic and Adult Fibroblast Cultures by Defined Factors. *Cell*, *126*(4), 663-676. https://doi.org/https://doi.org/10.1016/j.cell.2006.07.024

Tanaka, M., Chen, Z., Bartunkova, S., Yamasaki, N., & Izumo, S. (1999). The cardiac homeobox gene Csx/Nkx2.5 lies genetically upstream of multiple genes essential for heart development. *Development*, *126*(6), 1269-1280. https://doi.org/10.1242/dev.126.6.1269

Tanaka, M., Schinke, M., Liao, H. S., Yamasaki, N., & Izumo, S. (2001). Nkx2.5 and Nkx2.6, homologs of Drosophila tinman, are required for development of the pharynx. *Molecular and Cellular Biology*, *21*(13), 4391-4398. https://doi.org/10.1128/MCB.21.13.4391-4398.2001

Tanaka, M., Yamasaki, N., & Izumo, S. (2000). Phenotypic Characterization of the Murine Nkx2.6 Homeobox Gene by Gene Targeting. *Molecular and Cellular Biology*, *20*(8), 2874-2879. https://doi.org/10.1128/MCB.20.8.2874-2879.2000

Torroja, C., Gorfinkiel, N., & Guerrero, I. (2004). Patched controls the Hedgehog gradient by endocytosis in a dynamin-dependent manner, but this internalization does not play a major role in signal transduction. *Development*, *131*(10), 2395-2408. https://doi.org/10.1242/dev.01102

Tsai, P. T., Lee, R. A., & Wu, H. (2003). BMP4 acts upstream of FGF in modulating thymic stroma and regulating thymopoiesis. *Blood*, *102*(12), 3947-3953. https://doi.org/10.1182/blood-2003-05-1657

van Amerongen, R., & Berns, A. (2006). Knockout mouse models to study Wnt signal transduction. *Trends in Genetics*, *22*(12), 678-689. https://doi.org/https://doi.org/10.1016/j.tig.2006.10.001

Van Esch, H., Groenen, P., Nesbit, M. A., Schuffenhauer, S., Lichtner, P., Vanderlinden, G., Harding, B., Beetz, R., Bilous, R. W., Holdaway, I., Shaw, N. J., Fryns, J.-P., Van de Ven, W., Thakker, R. V., & Devriendt, K. (2000). GATA3 haplo-insufficiency causes human HDR syndrome. *Nature*, *406*(6794), 419-422. https://doi.org/10.1038/35019088

Van Kerckvoorde, M., Ford, M. J., Yeyati, P. L., Mill, P., & Mort, R. L. (2021). Live Imaging and Analysis of Cilia and Cell Cycle Dynamics with the Arl13bCerulean-Fucci2a BiosensorBiosensorsand Fucci Tools. In A. S. Coutts & L. Weston (Eds.), *Cell Cycle Oscillators : Methods and Protocols* (pp. 291-309). Springer US. https://doi.org/10.1007/978-1-0716-1538-6_21

Vincentz, J. W., Casasnovas, J. J., Barnes, R. M., Que, J., Clouthier, D. E., Wang, J., & Firulli, A. B. (2016). Exclusion of Dlx5/6 expression from the distal-most mandibular arches enables BMP-mediated specification of the distal cap. *Proc Natl Acad Sci U S A*, *113*(27), 7563-7568. https://doi.org/10.1073/pnas.1603930113

Vitelli, F., Morishima, M., Taddei, I., Lindsay, E. A., & Baldini, A. (2002). Tbx1 mutation causes multiple cardiovascular defects and disrupts neural crest and

cranial nerve migratory pathways. *Human Molecular Genetics*, *11*(8), 915-922. https://doi.org/10.1093/hmg/11.8.915

Vitelli, F., Morishima, M., Taddei, I., Lindsay, E., & Baldini, A. (2002). *Tbx1* mutation causes multiple cardiovascular defects and disrupts neural crest and cranial nerve migratory pathways. *Human Molecular Genetics*, *11*(8), 915-922.

Voitenleitner, C., Fanning, E., & Nasheuer, H. P. (1997). Phosphorylation of DNA polymerase alpha-primase by cyclin A-dependent kinases regulates initiation of DNA replication in vitro. *Oncogene*, *14*(13), 1611-1615. https://doi.org/10.1038/sj.onc.1200975

Wallin, J., Eibel, H., Neubüser, A., Wilting, J., Koseki, H., & Balling, R. (1996). Pax1 is expressed during development of the thymus epithelium and is required for normal T-cell maturation. *Development*, *122*(1), 23-30. https://doi.org/10.1242/dev.122.1.23

Wang, B., & Li, Y. (2006). Evidence for the direct involvement of βTrCP in Gli3 protein processing. *Proceedings of the National Academy of Sciences*, *103*(1), 33-38. https://doi.org/doi:10.1073/pnas.0509927103

Wang, F., Flanagan, J., Su, N., Wang, L. C., Bui, S., Nielson, A., Wu, X., Vo, H. T., Ma, X. J., & Luo, Y. (2012). RNAscope: a novel in situ RNA analysis platform for formalin-fixed, paraffin-embedded tissues. *J Mol Diagn*, *14*(1), 22-29. https://doi.org/10.1016/j.jmoldx.2011.08.002

Wang, R. N., Green, J., Wang, Z., Deng, Y., Qiao, M., Peabody, M., Zhang, Q., Ye, J., Yan, Z., Denduluri, S., Idowu, O., Li, M., Shen, C., Hu, A., Haydon, R. C., Kang, R., Mok, J., Lee, M. J., Luu, H. L., & Shi, L. L. (2014). Bone Morphogenetic

Protein (BMP) signaling in development and human diseases. *Genes & Diseases*, *1*(1), 87-105. https://doi.org/https://doi.org/10.1016/j.gendis.2014.07.005

Wei, Q., & Condie, B. G. (2011). A Focused In Situ Hybridization Screen Identifies Candidate Transcriptional Regulators of Thymic Epithelial Cell Development and Function. *PLoS One*, *6*(11), e26795. https://doi.org/10.1371/journal.pone.0026795

Xu, M., Sheppard, K. A., Peng, C. Y., Yee, A. S., & Piwnica-Worms, H. (1994). Cyclin A/CDK2 binds directly to E2F-1 and inhibits the DNA-binding activity of E2F-1/DP-1 by phosphorylation. *Mol Cell Biol*, *14*(12), 8420-8431. https://doi.org/10.1128/mcb.14.12.8420-8431.1994

Xu, P., Zheng, W., Laclef, C., Maire, P., Maas, R. L., Peters, M., & Xu, X. (2002). Eya1 is required for the morphogenesis of mammalian thymus, parathyroid, and thyroid. *Development*, *129*, 3033-3044.

Yagi, H., Furutani, Y., Hamada, H., Sasaki, T., Asakawa, S., Minoshima, S., Ichida, F., Joo, K., Kimura, M., Imamura, S.-i., Kamatani, N., Momma, K., Takao, A., Nakazawa, M., Shimizu, N., & Matsuoka, R. (2003). Role of TBX1 in human del22q11.2 syndrome. *The Lancet*, *362*(9393), 1366-1373. https://doi.org/10.1016/S0140-6736(03)14632-6

Zou, D., Silvius, D., Davenport, J., Grifone, R., Maire, P., & Xu, P.-X. (2006). Patterning of the third pharyngeal pouch into thymus/parathyroid by Six and Eya1. *Developmental Biology*, *293*(2), 499-512. https://doi.org/10.1016/j.ydbio.2005.12.015